

METHODS TO PERFORM SITE SPECIFIC SEISMIC HAZARD ASSESSMENT

A Dissertation Submitted in Partial Fulfillment of the requirement for the Award of the Degree of

Master of Engineering

In

Structural Engineering

Submitted By

Shubham Ranjan

802324019

M.E. Structural Engineering

Under The Guidance of

Dr. Pratik Tiwari

Assistant Professor

(Department of Civil Engineering)

Dr. Sumeet Mahajan

Joint General Manager

(RITES Ltd.)



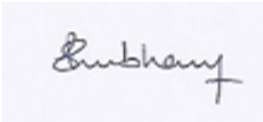
Department of Civil Engineering
Thapar Institute of Engineering & Technology
[Deemed to be University]
Patiala-147004 [Punjab]

JULY 2025

DECLARATION

I declare that the work which is presented in this seminar report entitled “**METHODS TO PERFORM SITE SPECIFIC SEISMIC HAZARD ASSESSMENT**” as per the requirement for the award of degree of **Master of Engineering, submitted** in the Department of Civil Engineering and Technology [TIET], Patiala. This work is carried out under the guidance and supervision of **Dr. Sumeet Mahajan** and **Dr. Pratik Tiwari**. It is declared that this work is original and has not been submitted anywhere else for the award of any other degree.

Date: 10-09-2025



Shubham Ranjan

802324019

CERTIFICATE

This is to certify that the Thesis entitled “METHODS TO PERFORM SITE SPECIFIC SEISMIC HAZARD ASSESSMENT” being submitted by SHUBHAM RANJAN (802324019), in partial fulfilment of the requirements for the award of degree of Master of Engineering in Structural Engineering at Thapar University, Patiala, is a Bonafide work carried out by the student under my supervision and guidance. The matter embodied in this report has not been submitted anywhere for award of any degree.



Dr. Pratik Tiwari
Assistant Professor
Department of Civil Engineering



Dr. Sumeet Mahajan
Joint General Manager
RITES Ltd.



राइट्स लिमिटेड
(भारत सरकार का प्रतिष्ठान)

RITES LIMITED

(Schedule 'A' Enterprise of Govt. of India)

RITES/HRD/36-03/2024-25/28

Dated: 11.02.2025

TO WHOMSOEVER IT MAY CONCERN

This is to certify that **Mr. Shubham Ranjan** student of **M.E (Structural Engineering)** at **Thapar Institute of Engineering & Technology** underwent internship in the **RCED Department** of **RITES Ltd.** for a period from **18.06.2024 – 18.12.2024.**

Mr. Shubham Ranjan shown keen interest in picking up various aspects related to the working of the division.

We wish him success for his future endeavors.

Mukesh
11/2/25

Mukesh Drolia

सहायक प्रबंधक (HR) प्रशिक्षण

Assistant Manager (HR)Trng.

दूरभाष: 0124-2728345/352/343

ईमेल: Mukesh.drolia@rites.com

Transforming to GREEN

कॉर्पोरेट कार्यालय: शिखर, प्लॉट नं. 1, सेक्टर-29, गुरुग्राम-122 001 (भारत), **Corporate Office:** Shikhar, Plot No. 1, Sector-29, Gurugram -122 001 (India)

पंजीकृत कार्यालय: स्कोप मीनार, लक्ष्मी नगर, दिल्ली-110092 (भारत), **Registered Office:** SCOPE Minar, Laxmi Nagar, Delhi-110092 (India)

दूरभाष, (Tel.): (0124) 2571666 फैक्स, (Fax): (0124) 2571660, ई-मेल (E-mail) info@rites.com वेबसाइट (Website): www.rites.com

CIN: L74899DL1974GOI007227



राइट्स लिमिटेड
(भारत सरकार का प्रतिष्ठान)
RITES LIMITED
(Schedule 'A' Enterprise of Govt. of India)

राइट्स/एचआरडी/36-03/2024-25/15
Date: 30.06.2025

TO WHOMSOEVER IT MAY CONCERN

This is to certify that **Mr. Shubham Ranjan** student of M.E (Structural Engineering) at Thapar Institute of Engineering & Technology, Patiala underwent internship in CEDS Department of RITES Ltd at Corp Office, Gurugram from 19th Dec 2024 to 19th June, 2025.

Mr. Shubham Ranjan has shown keen interest in picking up various aspects related to the working of the division.

We wish him success for his future endeavours.

धन्यवाद,

Warm Regards

शिवाक मित्तल/ Shivak Mittal
मुख्य प्रशिक्षण अधिकारी / Chief Training Officer
दूरभाष: 0124-2728343/345
ईमेल: Ctro@rites.com

Transforming to GREEN

कॉर्पोरेट कार्यालय: शिखर, प्लॉट नं. 1, सेक्टर-29, गुरुग्राम-122 001 (भारत), **Corporate Office:** Shikhar, Plot No. 1, Sector-29, Gurugram -122 001 (India)
पंजीकृत कार्यालय: स्कोप मीनार, लक्ष्मी नगर, दिल्ली-110092 (भारत), **Registered Office:** SCOPE Minar, Laxmi Nagar, Delhi-110092 (India)
दूरभाष, (Tel.): (0124) 2571666 फैक्स, (Fax): (0124) 2571660, ई-मेल (E-mail) info@rites.com वेबसाइट (Website): www.rites.com
CIN: L74899DL1974GOI007227

ACKNOWLEDGEMENT

I would like to extend my heartfelt gratitude to **Dr. Sumeet Mahajan, Joint General Manager in the department of Civil engineering design and Survey at RITES Ltd, Gurugram.** And **Dr. Pratik Tiwari, Assistant Professor in the Department of Civil Engineering and Technology, Patiala.** Their guidance, unwavering support, and motivation are significantly contributing to the success of my project. Dr. Sumeet Mahajan and Dr. Pratik Tiwari generously dedicated their valuable time to steering me in the right direction and provided insightful feedback on implementing my ideas. Their patient listening and constructive suggestions continuously inspired and propelled me forward throughout this endeavor. Additionally, I am thankful to the RITES Company and Thapar Institute for offering this opportunity, where I gained invaluable knowledge. Completing this report will enhance my technical skills, facilitated by the RITES and Thapar Institute's resources and assistance. Finally, I would like to thank my friends for their cooperation and support towards me for completing this report.

Dated: 10-09-2025

Shubham Ranjan

ABSTRACT

This dissertation, titled "**Methods to Perform Site Specific Seismic Hazard Assessment**," presents a comprehensive workflow for evaluating earthquake hazard through both deterministic and probabilistic approaches. Focusing on the Saraighat Bridge site in Guwahati, Assam, the study details the collection and homogenization of regional earthquake data, declustering procedures, and assignment of seismicity parameters to multiple fault sources via the Gutenberg-Richter relationship. Deterministic Seismic Hazard Analysis (DSHA) utilizes region-specific ground motion prediction equations to estimate conservative peak ground acceleration (PGA) values for each fault scenario, while Probabilistic Seismic Hazard Analysis (PSHA) quantifies the combined uncertainties and effects of all relevant seismic sources, generating hazard curves and uniform hazard spectra (UHS) across varied exceedance probabilities and design periods. The analysis demonstrates notable fault-specific hazard variability, with the Oldham Fault emerging as the controlling source for design-level ground motions at the study site. By benchmarking results against regional codes and prior studies, the research emphasizes the necessity of meticulous site-specific procedures for robust, performance-based seismic design in high-risk regions. The established methodology supports resilient infrastructure planning and enhanced seismic risk mitigation for critical facilities in Northeast India.

TABLE OF CONTENT

DECLARATION.....	II
CERTIFICATE.....	III
ACKNOWLEDGEMENT.....	VI
ABSTACT.....	VII
TABLE OF CONTENT.....	VIII
LIST OF FIGURES.....	X
LIST OF TABLES.....	XII
LIST OF EQUATIONS.....	XIII
CHAPTER 1	1
INTRODUCTION	1
1.1 Introduction	1
1.2 Introduction to Deterministic Seismic Hazard Analysis (DSHA)	2
1.3 Introduction to Probabilistic Seismic Hazard Analysis (PSHA)	2
1.4 Advantages of Site-specific Seismic Hazard Assessment	3
1.5 Problem Statement of the Project	4
1.6 Objectives of the study.....	5
CHAPTER 2	7
LITERATURE REVIEW	7
3.1 Summary of the Literature Review	43
3.2 Identified Research Gaps.....	43
3.3 Justification for Site-Specific Seismic Hazard Assessment	44
CHAPTER 3	45

METHODOLOGY FOR CASE STUDY	45
4.1 Introduction for Case Study.....	45
4.2 Data Collection	47
4.3 Declustering of Earthquake Catalogue.....	49
4.4 Completeness Analysis.....	49
4.5 Seismic Source Characterization	51
4.6 Assigning Earthquakes to each faults.....	54
4.7 Computation of seismic parameters.....	55
4.8 Estimation of Maximum Magnitude (M_{max}).....	58
4.9 Deterministic Seismic Hazard Assessment (DSHA)	62
4.10 Conclusion on DSHA results.	64
4.11 Probabilistic Seismic Hazard Assessment (PSHA).....	65
CHAPTER 4	73
CONCLUSION	73
REFERENCES	75
APPENDIX A	71
APPENDIX B	72

LIST OF FIGURES

Figure 1 Returning period versus magnitude charts for seismogenic zones SZ I–SZ X. The SZs with comparatively larger returning periods are indicated in [a], whereas the others 5 SZs are shown in (b) (Sharma, M.L., Malik, Shipra, 2006a).....	9
Figure 2 The probability vs. magnitude curves for (1)50 years, (2) 100 years, and (3)1000 years. The SZs are now classified into two categories according on their probability of occurrence. (Sharma, M.L., Malik, Shipra, 2006a).....	10
Figure 3 Histograms depicting the fluctuation of b-values observed and evaluated Mmax of seismogenic zones from SZ I to SZ X. (Sharma, M.L., Malik, Shipra, 2006a.).....	11
Figure 4 Histograms illustrating variation of , 10% exceedance in 50 years, and 20% exceedance in 50 years of seismogenic zones for SZ I to SZ X. (Sharma, M.L., Malik, Shipra, 2006a.).....	11
Figure 5 The spatial distribution of peak ground acceleration, as determined for each hypocentral (focus) depth range. (Nath & Thingbaijam, 2012)	14
Figure 6 Seismic hazard curves for selected cities (as stated on each plot) were derived for PGA and PSA at 0.2 and 1seconds, respectively, for a uniform firm rock site. (Nath & Thingbaijam, 2012)..	15
Figure 7 Seismic hazard distribution in India in terms of PGA and PSA at 0.2 and 0.1 seconds for firm rock sites, respectively. The maps also feature data of Nepal, Bhutan, Bangladesh and Sri Lanka. (Nath & Thingbaijam, 2012).....	17
Figure 8 Design response spectrum (5% dampened) for chosen cities. (Nath & Thingbaijam, 2012)	18
Figure 9 Seismic hazard curves at bedrock level for Agartala and Aizawl City. (Sil et al., 2013) ...	21
Figure 10 Uniform hazard spectrum at rock level for 2475 and 475 years of return periods in Agartala and Aizawl City. (Sil et al., 2013)	22
Figure 11 PGA (g) contours at bedrock level for 2 % and 10% likelihood of exceeding in 50 years. (Sil et al., 2013)	23

Figure 12 Contour maps of 2% exceedance in 50 years for: a) mean PGA, b) COV for mean PGA, c) Sa at 0.2 s, d) COV for Sa at 0.2, e) Sa at 1.0 s, and f) COV for Sa at 1.0 s. (Das et al., 2016).....	26
Figure 13 Seismic hazard curve of 12 district headquarters. (Bahuguna & Sil, 2020)	32
Figure 14 The following district headquarters' PGA values were compared using DSHA. (Bahuguna & Sil, 2020).....	34
Figure 15 Comparison of the PGA values for district headquarters computed using PSHA for a 2% probability in 50 years. (Bahuguna & Sil, 2020)	35
Figure 16 The mean and quantile UHS for various cities at 10% POE in 50 years are on the right, while the mean hazard curves calculated for a variety of spectral periods, including PGA, are on the left. (Bahuguna & Sil, 2020).....	38
Fig. 17 Guwahati city's ground level spectra (5% damped) for over 2500 years and 10,000 years, respectively . (Bandyopadhyay et al., 2022).....	41
Figure 18 Faults and their distance from Saraighat Bridge.....	48
Figure 19 Plot of Data Completeness by CUVI method.....	50
Figure 20 Comparison of Length and Depth of Considered Seismic Sources.....	53
Figure 21 G - R Plots for each fault.....	58
Figure 22 DSHA result for different Faults.....	63
Figure 23 Seismic Hazard Curve for Saraighat Bridge	68
Figure 24 Fault-Wise PGA for Multiple Exceedance Probabilities.....	69
Figure 25 Uniform Hazard Spectrum (UHS) for the Oldham Fault at five return periods (475, 950, 975, 1975, and 2475 years), developed from PSHA and scaled using IS 1893 spectral shape for rock sites.	70

LIST OF TABLES

Table 1 Seismicity parameters calculated for each zone. (Sil et al., 2013).	20
Table 2 Seismic Zone Factor Z.(IS 1893:2016 Part I, 2016).....	29
Table 3 Seismicity parameters of fault/lineaments.(Bahuguna & Sil, 2020)	31
Table 4 Seismic hazard curve of 12 district headquarters.(Bahuguna & Sil, 2020)	33
Table 5 The PGA value contrasts with other research for the PSHA approach (10% in 50 years). ..	43
Table 6 Details of various faults considered in the study.	52
Table 7 Calculated a & b Value.....	57
Table 8 Estimation of Mmax Values.	59
Table 9 Mmax and Mmin values of faults.	60
Table 10 Values of PGA for each fault at bedrock.....	63
Table 11 Final values of PGA calculated for each fault after amplification (Surface)	63
Table 12 Fault Wise PGA for multiple exceedance Probabilities.	71

LIST OF EQUATIONS

Equation 1 Empirical relationship developed by Sitharam & Sil ,2014.	47
Equation 2 Gutenberg-Richter (G-R) law.(Beitr, n.d.).....	55
Equation 3 NDMA (2011) GMPE.....	61
Equation 4 Bajaj & Anbazhagan (2019) GMPE	61
Equation 5 Hazard Integration (kramer, n.d.)	67

CHAPTER 1

INTRODUCTION

1.1 Introduction

Creating secure and resilient infrastructure in areas susceptible to earthquakes necessitates a comprehensive understanding of local seismic threats. While regional seismic maps provide a broad overview of earthquake risk, they frequently overlook the specific geological and soil attributes that can greatly influence ground shaking at a given site. To tackle these unique site-related factors, engineers and researchers utilize Site-Specific Seismic Hazard Assessment (SSSHA), which offers customized predictions of potential earthquake effects for specific locations. SSSHA primarily depends on two analytical methods: Deterministic Seismic Hazard Analysis (DSHA) and Probabilistic Seismic Hazard Analysis (PSHA). DSHA focuses on the impacts of a single, significant earthquake scenario typically the largest credible event that could occur on the nearest active fault. This approach yields a conservative estimation of ground motion, ensuring that essential structures are engineered to endure the most intense plausible event. Conversely, PSHA assesses the likelihood that different levels of ground shaking will exceed at a site over a specified timeframe. By factoring in all possible seismic sources, their probabilities of occurrence, and ground motion models, PSHA incorporates the uncertainties associated with earthquake activity and ground response. This probabilistic viewpoint allows for the design of structures that can satisfy safety standards throughout their operational lifespan. By integrating DSHA and PSHA, site-specific seismic hazard assessments provide a solid framework for comprehending and reducing earthquake risks, ultimately aiding the construction of safer and more resilient buildings and infrastructure in at-risk regions.

1.2 Introduction to Deterministic Seismic Hazard Analysis (DSHA)

Deterministic Seismic Hazard Analysis (DSHA) is a key technique employed in earthquake engineering to assess the expected ground shaking at a particular site due to a specific earthquake scenario. In contrast to probabilistic methods that evaluate various possible earthquakes and their probabilities, DSHA concentrates on the most significant event + usually the largest credible earthquake that could occur on the nearest or most impactful fault affecting the location. The DSHA methodology includes identifying pertinent seismic sources, determining the maximum magnitude that each source might produce, and estimating the associated ground motions at the site of interest. This approach is especially important for the design of critical infrastructure such as bridges, hospitals, and nuclear facilities, where prioritizing safety against the most severe plausible event is essential. By focusing on a worst-case scenario, DSHA offers engineers and decision-makers a conservative foundation for structural design and risk management. Although it does not consider the likelihood of occurrence, DSHA continues to be an essential tool for protecting vital structures from extreme seismic events.

1.3 Introduction to Probabilistic Seismic Hazard Analysis (PSHA)

Probabilistic Seismic Hazard Analysis (PSHA) is a detailed method utilized to assess earthquake risks by taking into account the entire range of possible seismic events and their related uncertainties. In contrast to deterministic approaches that concentrate on a single, extreme scenario, PSHA consolidates data from all potential earthquake sources, their probability of occurrence, and the variety of ground motions they could trigger. The process of PSHA includes identifying significant faults and seismic areas, forecasting the frequency and magnitude of possible earthquakes, and employing

ground motion prediction models to evaluate the anticipated shaking at a particular location. By integrating these elements, PSHA computes the likelihood that different levels of ground shaking will be surpassed over a specified duration, such as 50 or 100 years. This probabilistic approach allows engineers and planners to design buildings that align with defined safety and performance goals throughout their anticipated lifetimes. PSHA is particularly useful for risk-informed decision-making, as it presents a more comprehensive view of seismic hazards by considering the intrinsic uncertainties associated with earthquake occurrences and ground reactions. Consequently, PSHA has become a crucial resource in contemporary seismic design regulations and hazard evaluations for essential infrastructure and urban development.

1.4 Advantages of Site-specific Seismic Hazard Assessment

- **Improves Structural Safety** – Provides accurate ground motion inputs for earthquake-resistant design.
- **Supports Risk Reduction** – Helps minimize loss of life and property by identifying high-risk areas.
- **Enables Site-Specific Design** – Accounts for local soil, fault proximity, and seismic conditions.
- **Guides Code Development** – Forms the basis for seismic design standards and building codes.
- **Aids Performance-Based Design** – Supplies ground motion values for different return periods.
- **Cost-Effective** – Balances safety with economic design by avoiding over- or underestimation.
- **Helps in Planning** – Assists in land-use decisions, emergency planning, and hazard zoning.
- **Insurance & Finance** – Used in risk modeling for earthquake insurance and premium setting.
- **Encourages Collaboration** – Combines inputs from multiple scientific and engineering fields.

- **Raises Awareness** – Informs communities and promotes resilience against seismic hazards.

1.5 Problem Statement of the Project

India's northeastern region is known for its seismic activity due to the intricate interactions between the Indian and Eurasian tectonic plates. Nevertheless, numerous vital infrastructure developments such as bridges, highways, and essential structures still depend on generalized seismic zoning maps for their design, which fail to consider local geological circumstances, proximity to faults, or site-specific amplification effects. Consequently, critical facilities may be either excessively designed, resulting in unnecessary expenses, or insufficiently designed, which poses significant safety threats during seismic events. The absence of thorough and location-specific hazard evaluations adds uncertainty to the prediction of ground motion parameters essential for performance-based and resilient infrastructure development. Although both Deterministic Seismic Hazard Analysis (DSHA) and Probabilistic Seismic Hazard Analysis (PSHA) are recognized methods for assessing hazards, there is often misunderstanding regarding their use, data needs, and limitations. Furthermore, several areas in India do not have extensive fault databases, region-specific Ground Motion Prediction Equations (GMPEs), or cohesive workflows for performing Site-Specific Seismic Hazard Assessments (SSSHA). This dissertation seeks to fill these gaps by investigating the techniques utilized in site-specific seismic hazard assessments and showcasing their practical implementation through a case study of the **Saraighat Bridge in Guwahati, Assam**. The objective is to develop a clear, step-by-step approach that integrates seismic source characterization, suitable ground motion models, and local site conditions to generate dependable and actionable hazard estimates.

1.6 Objectives of the Study

This study aims to perform integrated Deterministic and Probabilistic Seismic Hazard Assessments (DSHA and PSHA) for a critical site located in a region of extreme seismic activity. The research employs the following methodological approach:

Phase 1: Seismic Source Characterization

1. **Source Identification:** Map and characterize nearby active seismic sources (faults and tectonic features) using regional geological records and seismological data.
2. **Seismic Catalogue Refinement:** Process historical earthquake records through declustering techniques to remove dependent events and isolate primary seismicity patterns.

Phase 2: Deterministic Seismic Hazard Assessment (DSHA)

3. **Recurrence Modeling:** Quantify seismicity parameters by applying the Gutenberg-Richter recurrence law.
4. **Ground Motion Prediction:** Select and adapt suitable Ground Motion Prediction Equations (GMPEs) to simulate shaking for multiple earthquake scenarios.
5. **Critical Parameter Extraction:** Compute key ground motion metrics (e.g., Peak Ground Acceleration) for the dominant seismic source.

Phase 3: Probabilistic Seismic Hazard Assessment (PSHA)

6. **Hazard Curve Development:** Compute the annual rate of exceedance and generate seismic hazard curves reflecting probabilities of different ground motion levels over specified return periods
7. **Uniform Hazard Spectra (UHS):** Develop UHS plots for various return periods (e.g., 475, 2475 years) to support structural design and seismic risk assessment.
8. **Validation and Comparison:** Compare obtained hazard values with national code (IS 1893:2016) and previous studies to assess hazard level deviations and consistency

CHAPTER 2

LITERATURE REVIEW

Sharma, M.L., Malik, Shipra, 2006a. A detailed seismic hazard assessment has been carried out for the northeastern region of India by analyzing both the comprehensive and critical sections of the regional earthquake dataset. The study area has been categorized into four principal seismogenic sources: (1) the major Himalayan fault systems, including the Main Boundary Thrust (MBT) and Main Central Thrust (MCT); (2) the Eastern Syntaxis; (3) the Shillong Massif; and (4) the north–south trending Arakan Yoma seismic belt.

To enable more refined hazard modeling, these four broad seismic sources have been subdivided into ten distinct seismogenic zones, each based on specific tectonic and structural characteristics. These zones are defined as follows:

- **SZ I:** Eastern Himalaya (East–West trending features)
- **SZ II:** Eastern Syntaxis
- **SZ III:** Shillong Plateau (a section of the Shillong Massif)
- **SZ IV:** Dauki Fault (part of Shillong Massif)
- **SZ V:** Sylhet Fault (part of Shillong Massif)
- **SZ VI:** Naga Disang Thrust (North–South trending fault)
- **SZ VII:** Eastern Boundary Thrust I
- **SZ VIII:** Eastern Boundary Thrust II
- **SZ IX:** Eastern Boundary Thrust III

- **SZ X:** Mat Fault (all part of North–South trending structures)

Probabilistic Seismic Hazard Analysis (PSHA) was performed individually for each of these ten zones. The recurrence intervals for different earthquake magnitudes within these zones are presented in Figure 1. Specifically, Figure 1(a) reveals that zones SZ I, III, V, VI, and X show longer recurrence intervals for magnitude 6 earthquakes, whereas zones SZ II, IV, VII, VIII, and IX (Figure 1(b)) exhibit comparatively shorter recurrence periods.

For a 10% chance of exceedance in 50 years, Peak Ground Acceleration (PGA) values across the zones range between 0.05g and 0.6g. On the other hand, with a 20% probability of exceedance over the same time frame, the PGA values are observed to decrease and fall within the range of 0.01g to 0.4g.

Figures 2(a), 2(b), and 2(c) illustrate the probabilities of various magnitude earthquakes occurring over return periods of 50, 100, and 1000 years, respectively. Meanwhile, Figure 3 compares the observed and predicted maximum magnitudes across different zones, highlighting discrepancies, with the most significant deviation found in Zone II.

The b-values, which quantify the statistical relationship between earthquake frequency and magnitude, are calculated for all zones. The highest b-value is identified in SZ III, whereas the lowest appears in SZ VI. Figure 4 presents the maximum expected magnitudes in each zone under 10% and 20% probability of exceedance. Additionally, the l-values, representing the rate of seismic events, are lowest in SZ V and VI, and highest in SZ VIII, suggesting a higher frequency of lower-magnitude events in that zone.

Notably, the most significant probable earthquake magnitudes associated with both 10% and 20% exceedance levels are predominantly linked to Zone IV (Dauki Fault).

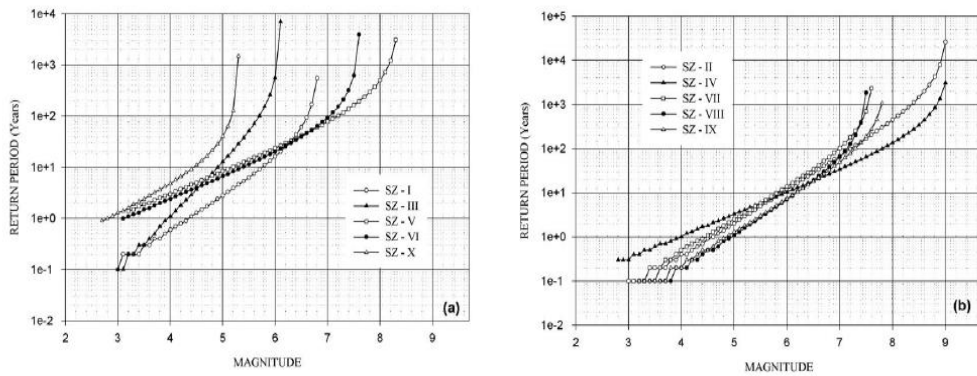


Figure 1 Returning period versus magnitude charts for seismogenic zones SZ I–SZ X. The SZs with comparatively larger returning periods are indicated in [a], whereas the others 5 SZs are shown in (b) (Sharma, M.L., Malik, Shipra, 2006a)

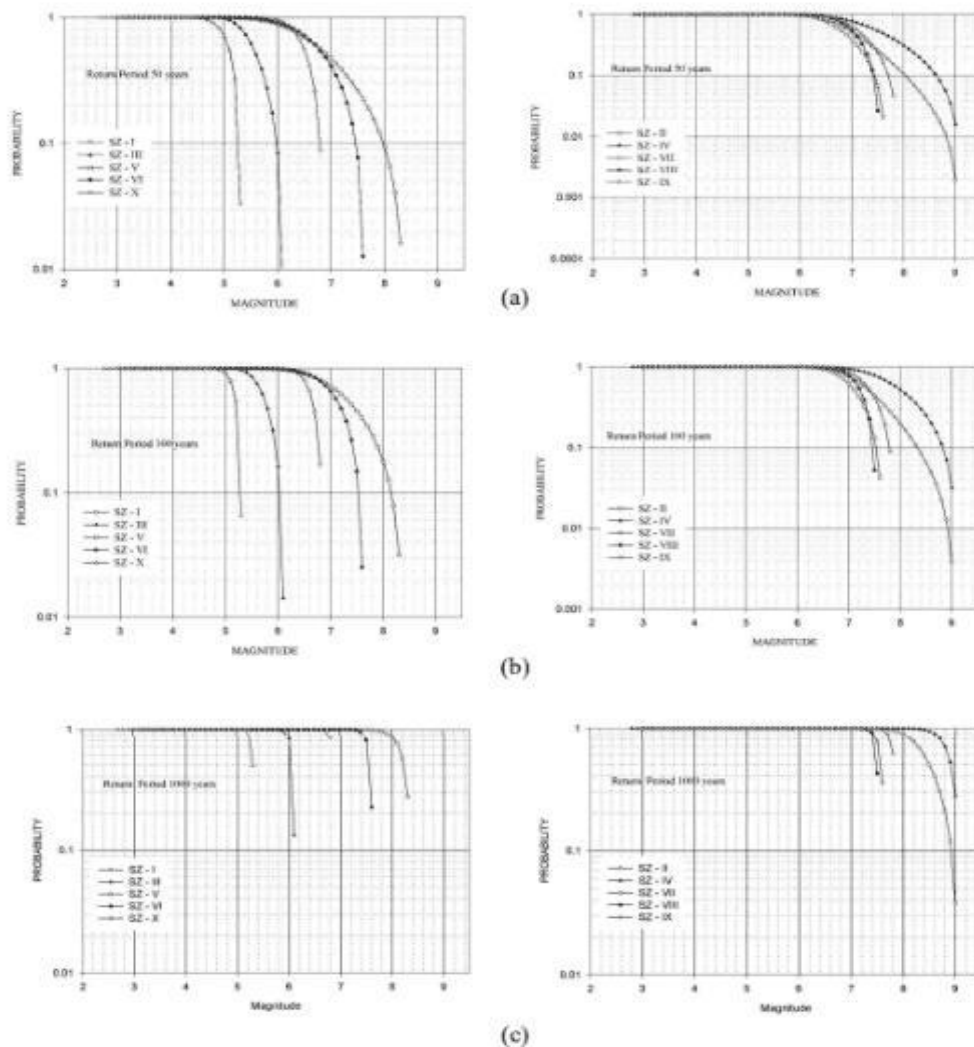


Figure 2 The probability vs. magnitude curves for (1)50 years, (2) 100 years, and (3)1000 years. The SZs are now classified into two categories according on their probability of occurrence. (*Sharma, M.L., Malik, Shipra, 2006a*)

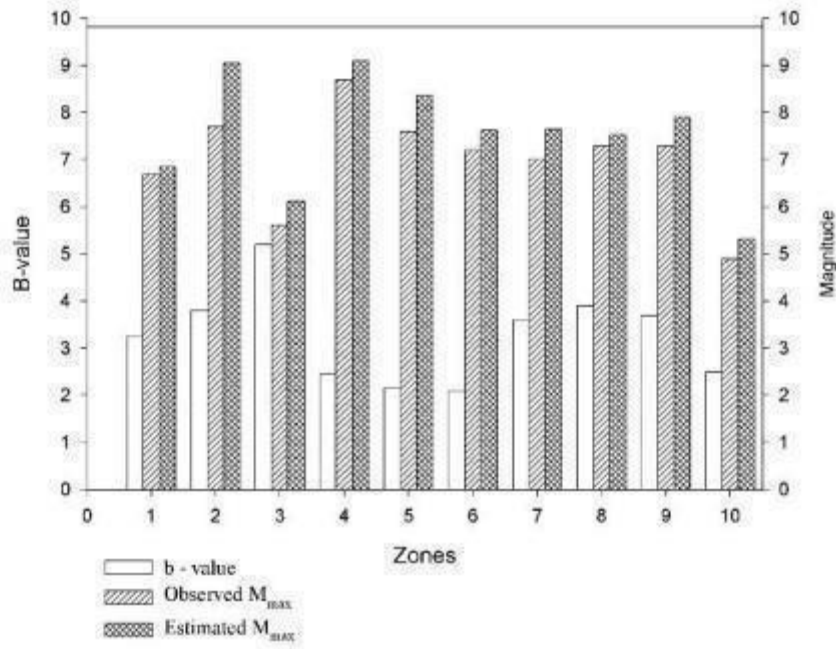


Figure 3 Histograms depicting the fluctuation of b-values observed and evaluated M_{max} of seismogenic zones from SZ I to SZ X. (Sharma, M.L., Malik, Shipra, 2006a.)

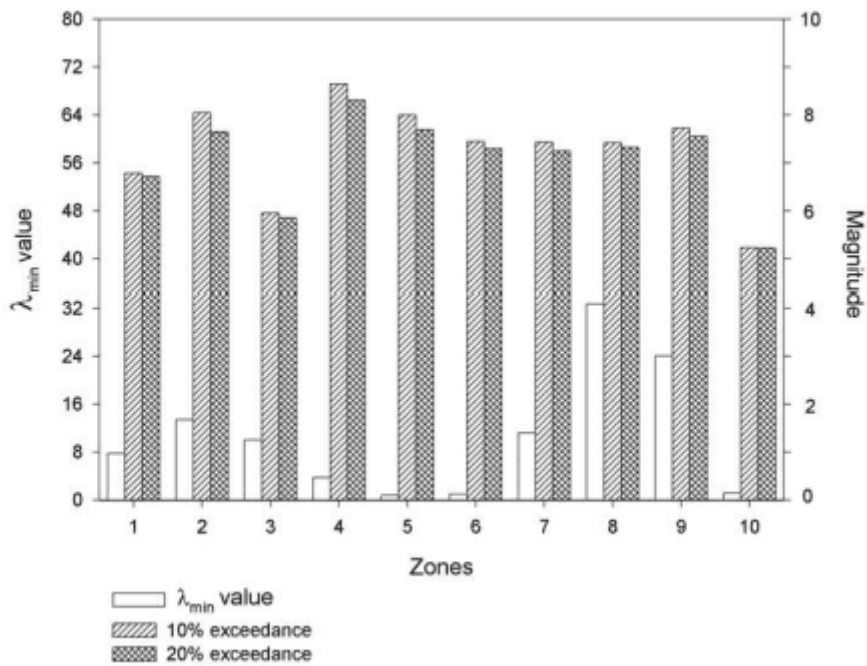


Figure 4 Histograms illustrating variation of λ_{min} value, 10% exceedance in 50 years, and 20% exceedance in 50 years of seismogenic zones for SZ I to SZ X. (Sharma, M.L., Malik, Shipra, 2006a.)

A variety of research has explored the seismic risks in this region, including investigations by Kaila et al. (1972), Rao and Rao (1979), Gupta and Srivastava (1990), Shanker and Sharma (1997, 1998), Arora and Sharma (1998), Bhatia et al. (1999), and Sharma and Shanker (2001). According to Shanker and Sharma (1998), the area is classified into Zones V and VI, which represent Northeast India (NEI) and the Burma-Andaman-Nicobar (BAN) region, respectively. Their study estimated the maximum potential earthquake magnitudes (M_{max}), R_6 , and b-values for NEI as 8.5, 7, and 1.89 ± 0.15 , and for BAN as 9.2, 5, and 1.49 ± 0.12 . In contrast, Rao and Rao (1979) found b-values of 1.66 for NEI and 1.93 for BAN, while Kaila et al. (1972) reported that the b-value ranged from 0.7 to 1.3 for NEI and from 0.8 to 1.3 for BAN. Gupta and Srivastava (1990) provided $R_{6.0}$ values of 4.44 for NEI and 3.97 for BAN. Shanker and Sharma (1997) utilized maximum likelihood estimation to identify important seismic hazard parameters for NEI, presenting M_{max} , b, beta, and lambda as 9.20, 0.92 ± 0.05 , 2.16 ± 0.12 , and 6.70 ± 0.61 , respectively. Arora and Sharma (1998) employed artificial neural networks to further evaluate seismic hazards in Northeast India, segmenting the region into four unique seismogenic zones. Their qualitative evaluation indicated the existing potential for earthquakes in the area. Numerous studies also propose that the energy accumulation cycle for seismic activities in this region is approaching its conclusion, suggesting a significant release of seismic energy and consequently a greater risk of large earthquakes within the forthcoming 30 to 50 years.

(Nath & Thingbaijam, 2012) This research presents an extensive seismic hazard assessment for India, considering the country's complex tectonic framework and diverse seismic activity patterns. By creating a detailed catalogue of earthquakes and integrating comprehensive seismotectonic information along with ground motion prediction equations (GMPEs), the study assesses hazard levels nationwide with considerable precision. A key outcome of this investigation is the creation of seismic hazard maps that illustrate peak ground acceleration (PGA) values for various return periods, essential for pinpointing higher-risk areas.

The results emphasize that the Himalayan region and northeastern India are notably vulnerable to increased seismic hazards. A detailed analysis of PGA distribution, particularly in these active regions, shows that both shallow (0–25 km) and deeper crustal earthquakes (25–70 km) significantly influence the hazard profile. Specifically, the west-central Himalayas and northeastern India are impacted by heightened hazard contributions from deeper crustal strata. Furthermore, intraslab earthquakes occurring within the Indo-Myanmar arc at depths ranging from 70 to 180 km are identified as significant contributors to seismic risk in northeastern India. Western Kashmir also raises concerns, as it faces seismic threats from both shallow crustal and subduction-related events. Although this study does not provide extensive detail, the Andaman-Nicobar Islands are acknowledged as locations where both shallow and deep-seated seismic hazards exist.

The spatial distribution of PGA, depicted in Figure 8 of the cited study, is derived from smoothed-gridded seismicity source zonations and offers a thorough overview of the hazard landscape, specifically for a 10% probability of exceedance over the forthcoming 50 years. These findings are crucial for shaping earthquake-resistant design standards and disaster risk mitigation strategies, ensuring that infrastructure

development and emergency preparedness in India are informed by current scientific insights on seismic risk.

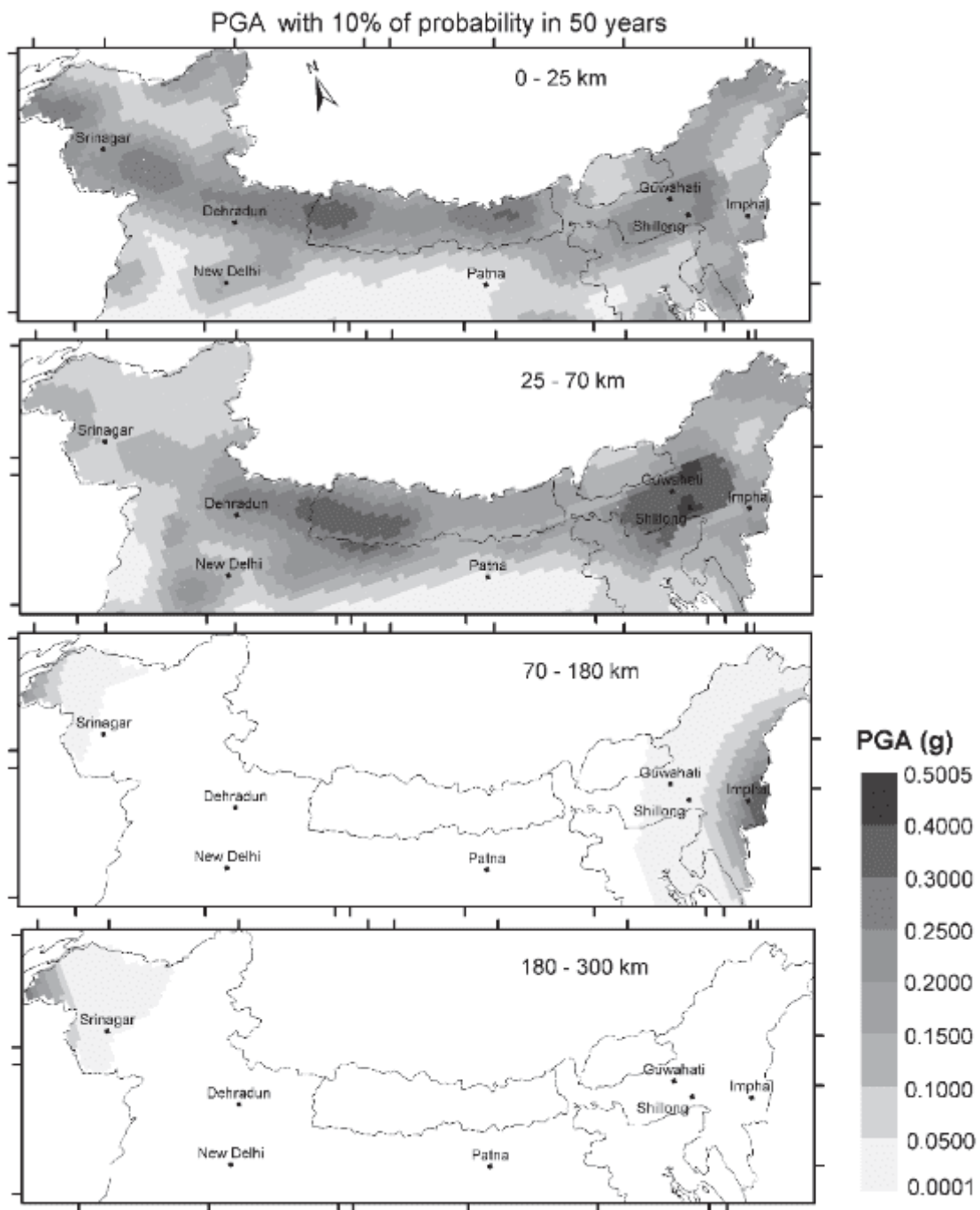


Figure 5 The spatial distribution of peak ground acceleration, as determined for each hypocentral (focus) depth range. (Nath & Thingbaijam, 2012)

The calculations correspond to a return period of 475 years and are exclusively based on smooth-gridded seismicity source zonation. By integrating findings from various

depth segments, we have successfully established overall hazard distributions. Figure 6 displays hazard curves for key cities and is supported by additional data, whereas Figure 10 depicts seismic hazard maps. These maps illustrate the spatial distributions of Peak Ground Acceleration (PGA) and pseudo-spectral acceleration (PSA) for periods of 0.2 seconds and 1 second, computed with exceedance probabilities of 10% and 2% over 50 years. These probabilities correspond to return periods of 475 and 2,475 years, respectively. The analysis reveals that tectonically active areas such as the Garhwal Himalayas, western Kashmir, and northeastern India encounter heightened hazards. Additionally, stable continental areas, which include western Gujarat, the Koyna-Warna region, and urban centres like Delhi, Jabalpur, Satpura, Latur, and the Bengal basin, also demonstrate increased risks.

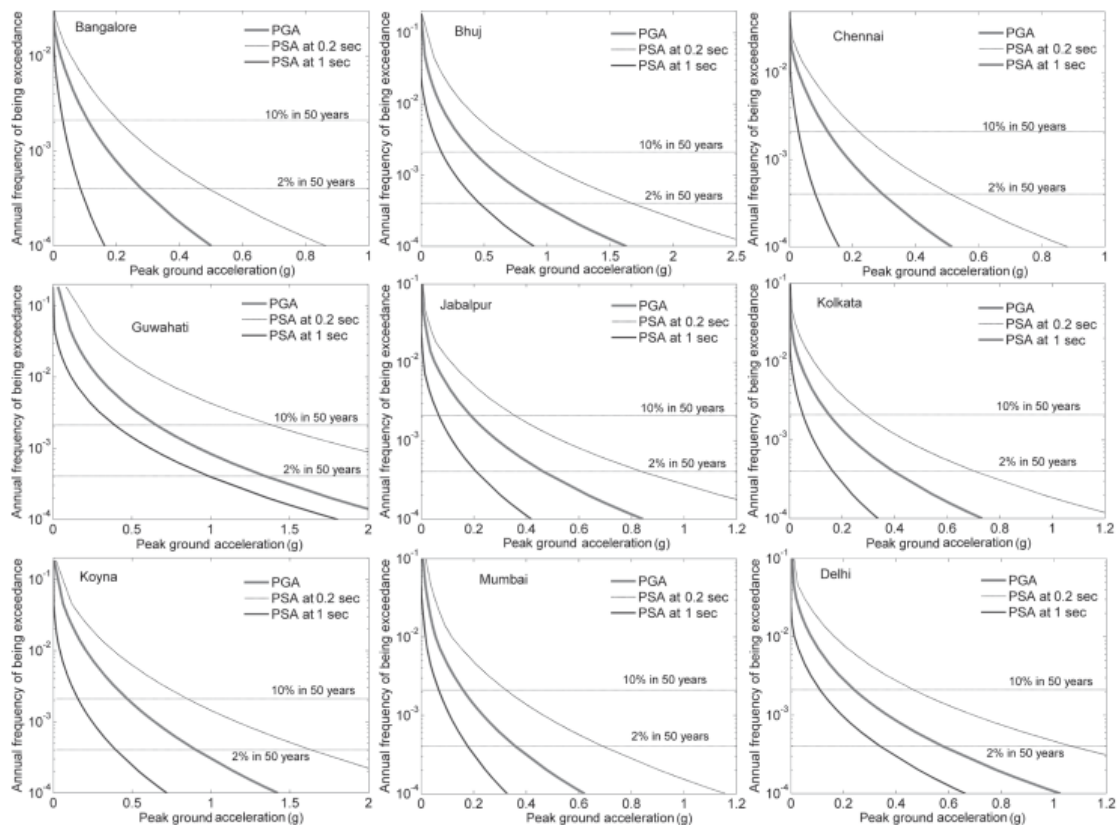


Figure 6 Seismic hazard curves for selected cities (as stated on each plot) were derived for PGA and PSA at 0.2 and 1 seconds, respectively, for a uniform firm rock site. (Nath & Thingbaijam, 2012)

The reviewed study also compares computed PGA values with those outlined by BIS (2002), GSHAP, and earlier analyses. The results indicate higher hazard levels,

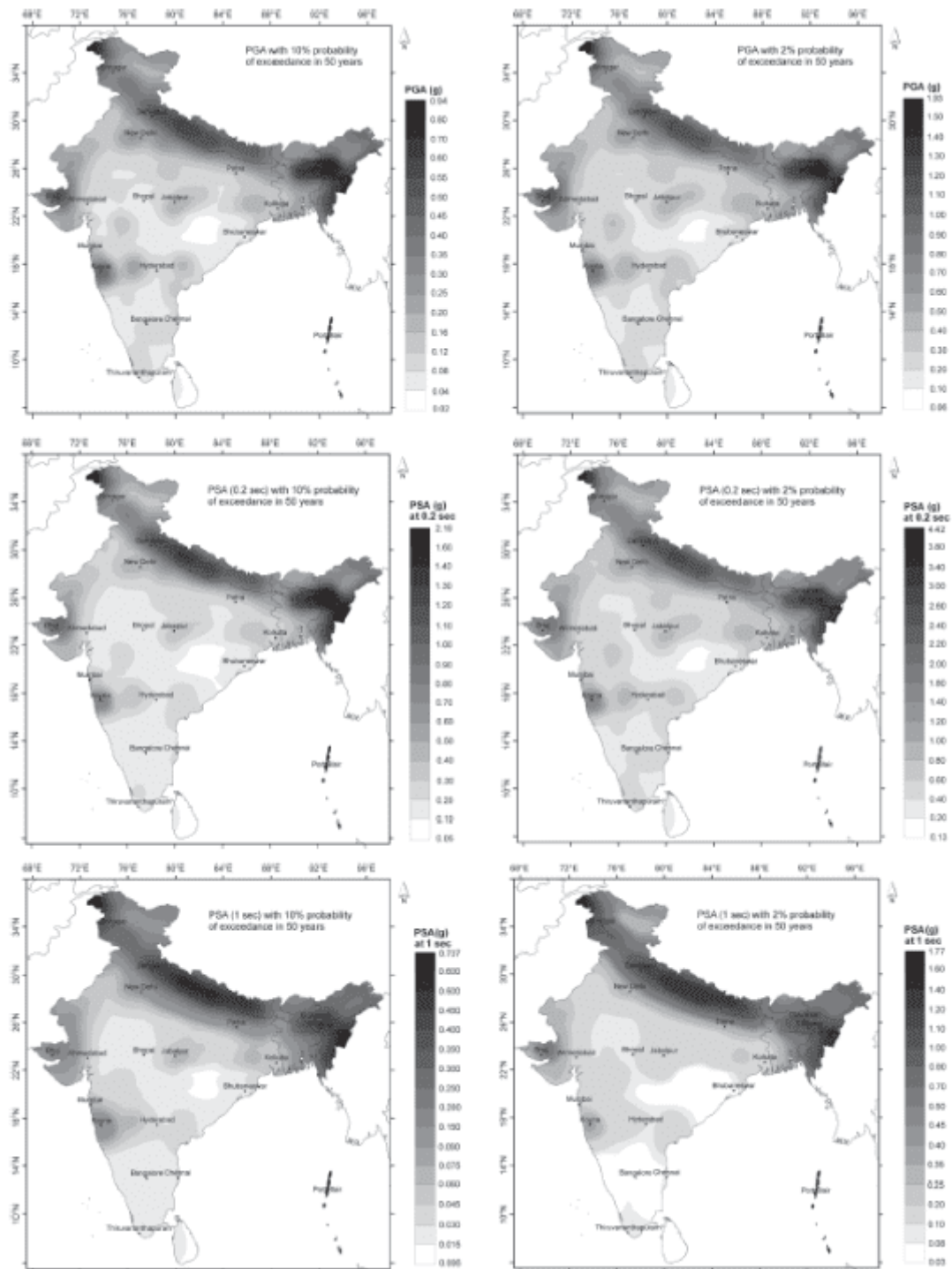


Figure 7 Seismic hazard distribution in India in terms of PGA and PSA at 0.2 and 0.1 seconds for firm rock sites, respectively. The maps also feature data of Nepal, Bhutan, Bangladesh and Sri Lanka. (*Nath & Thingbaijam, 2012*)

particularly in areas prone to seismic activity, with some differences in regional calculations. For example, Mahajan et al. (2010) documented a peak PGA of 0.75 g in the northwestern Himalayas, whereas the current analysis indicates a maximum of 0.60 g for this region. In northeastern India, the findings reveal hazard values that are 1.3 to 2.0 times greater than those predicted by Sharma and Malik (2006).

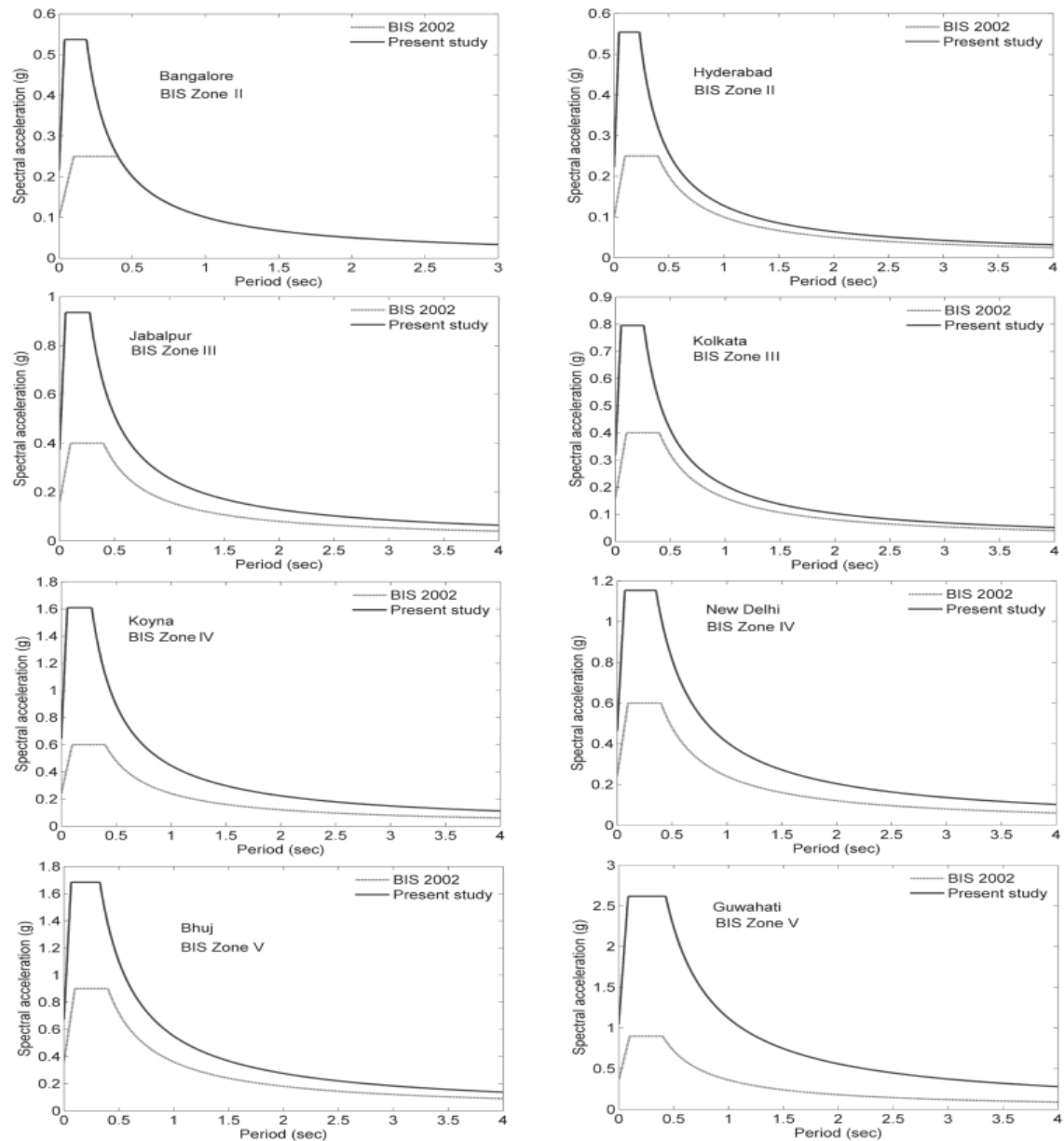


Figure 8 Design response spectrum (5% dampened) for chosen cities. (Nath & Thingbaijam, 2012)

To evaluate updated seismic hazard analysis relative to current standards, eight cities, representing different seismic zones as per BIS (2002), were selected. Design response spectra at 5% damping for firm rock site conditions were plotted for these locations (Figure 8). The analysis employed PSA values at 0.2 seconds and 1 second for a 2,475-year return period, in alignment with the International Building Code (IBC 2006, 2009). This comprehensive review underscores the importance of integrating advanced seismic hazard modelling with regional and site-specific analyses for improved risk management and building code compliance.

(*Sil et al., 2013*) An extensive literature survey on seismic hazard assessment has been undertaken, emphasizing notable research contributions aimed at evaluating ground motion at the bedrock level in earthquake-prone areas. A key study specifically investigates the Probabilistic Seismic Hazard Assessment (PSHA) for the northeastern Indian states of Tripura and Mizoram.

In this study, earthquake data were compiled for the period from 1731 to 2010, encompassing seismic events within a 500 km radius surrounding the borders of these two states. The earthquake catalogue was carefully processed through a declustering procedure, which removed dependent events such as foreshocks and aftershocks by applying spatial and temporal filtering methods. Following this, a statistical completeness analysis was carried out to verify the reliability and sufficiency of the dataset.

Subsequently, seismicity parameters including the 'a' and 'b' values were determined for each identified source zone, with the results documented in Table 1. Individual hazard curves for six major seismic sources were developed and then integrated to form a combined hazard curve, which captures the cumulative seismic threat posed by all contributing sources.

Figures 9a and 9b depict the bedrock-level hazard curves for the cities of Agartala and Aizawl, respectively. Among the analysed zones, the IBR zone emerged as the most seismically active, followed by the SP and BB zones. These zones demonstrated relatively higher annual earthquake occurrence rates and greater levels of ground acceleration compared to the remaining areas within the study scope.

Table 1 Seismicity parameters *a* and *b* values calculated for each zone. (Sil et al., 2013).

Sl. No.	Seismic regions/zones	Parameter- (<i>a</i>) value	Parameter- (<i>b</i>) value	R^2 (coefficient of correlation)
1	Indo-Burma range (IBR)	4.94	0.79	0.96
2	Eastern Himalaya (EH)	4.88	0.86	0.92
3	Shillong Plateau (SP)	3.28	0.61	0.98
4	Bengal Basin (BB)	3.03	0.61	0.93
5	Naga Thrust (NT)	2.57	0.54	0.94
6	Mishmi Thrust (MT)	2.54	0.54	0.90

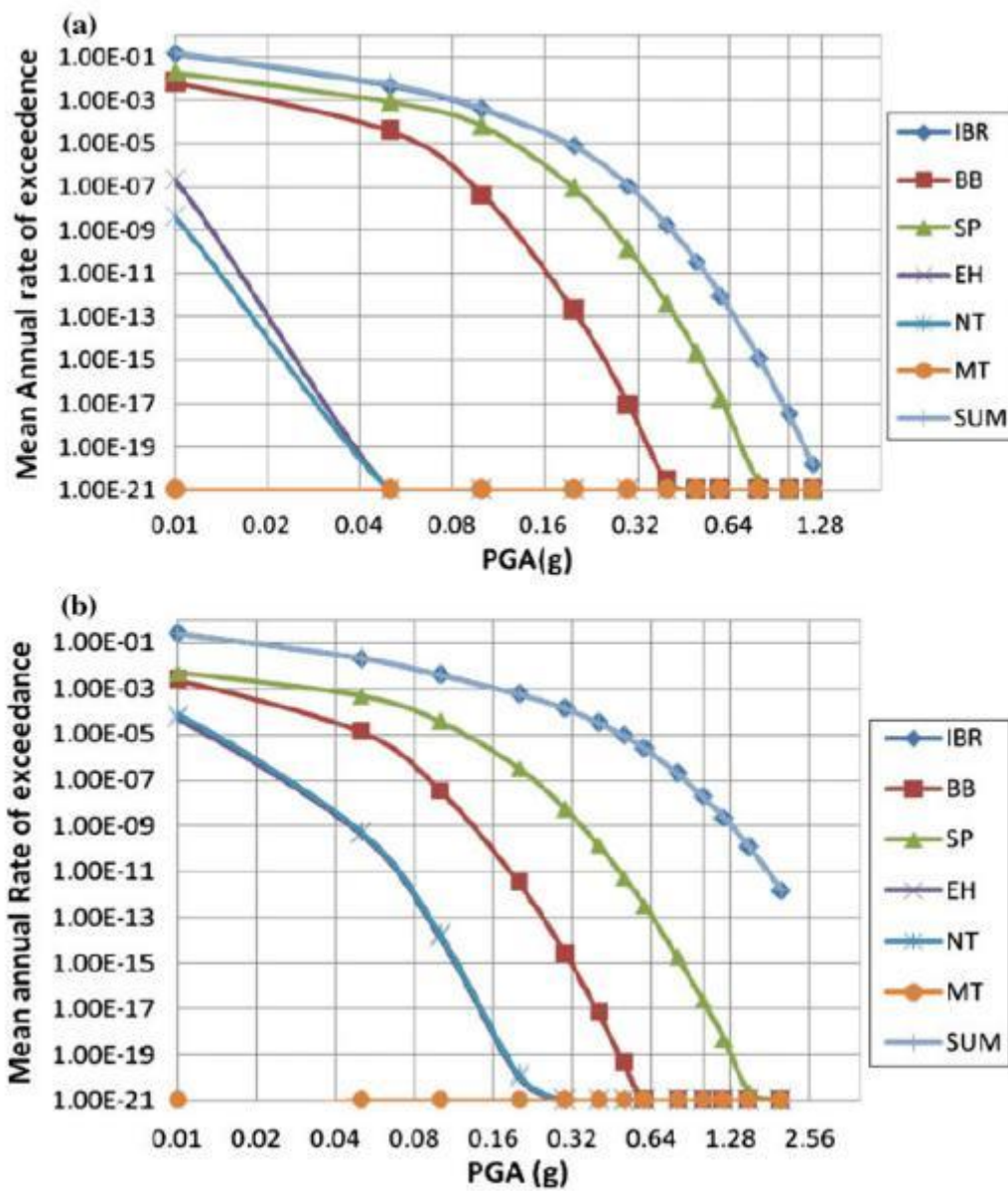


Figure 9 Seismic hazard curves at bedrock level for Agartala and Aizawl City. (Sil et al., 2013)

Figures 10a and 10b illustrate the equivalent UHS for Agartala and Aizawl. PGA values were determined at each grid point to assess the seismic risk at the bedrock level. The PGA distribution maps presented in Figures 10a and 10b represent the likelihood of exceedance at 2% and 10% within a 50-year timeframe, respectively. In Tripura, PGA measurements vary from 0.06 to 0.5 g for a 2% likelihood and from 0.03 to 0.26 g for a 10% chance. Likewise, in Mizoram, the PGA values span from 0.11 to 0.4 g for a 2% probability and from 0.08 to 0.23 g for a 10% probability. The highest PGA readings in Tripura were recorded in the northern region, exceeding 0.46 g and 0.26 g for the respective return periods.

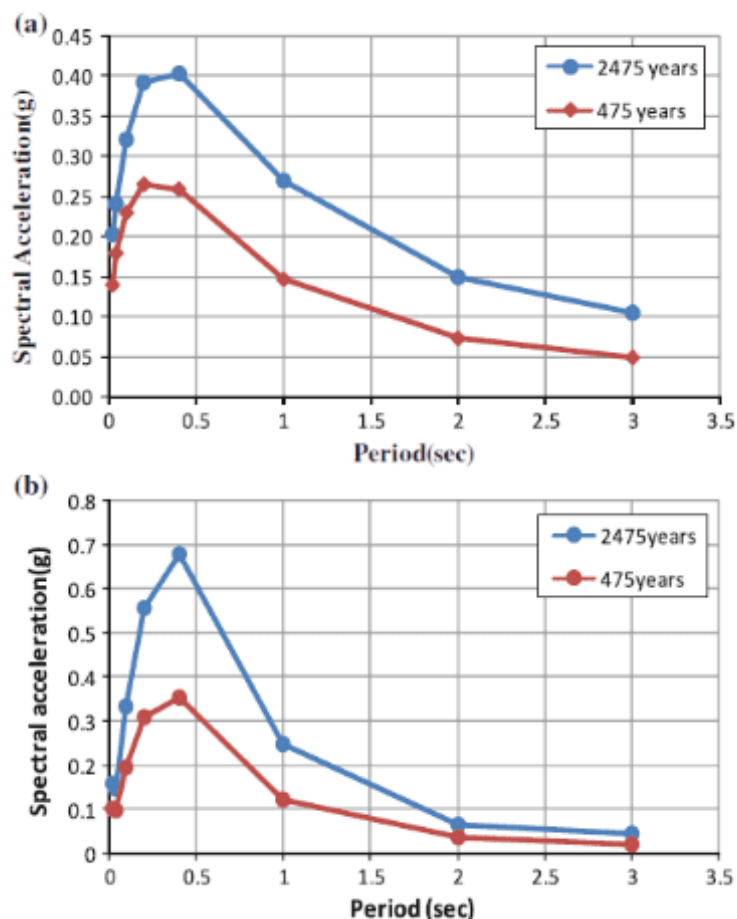


Figure 10 Uniform hazard spectrum at rock level for 2475 and 475 years of return periods in Agartala and Aizawl City. (Sil et al., 2013)

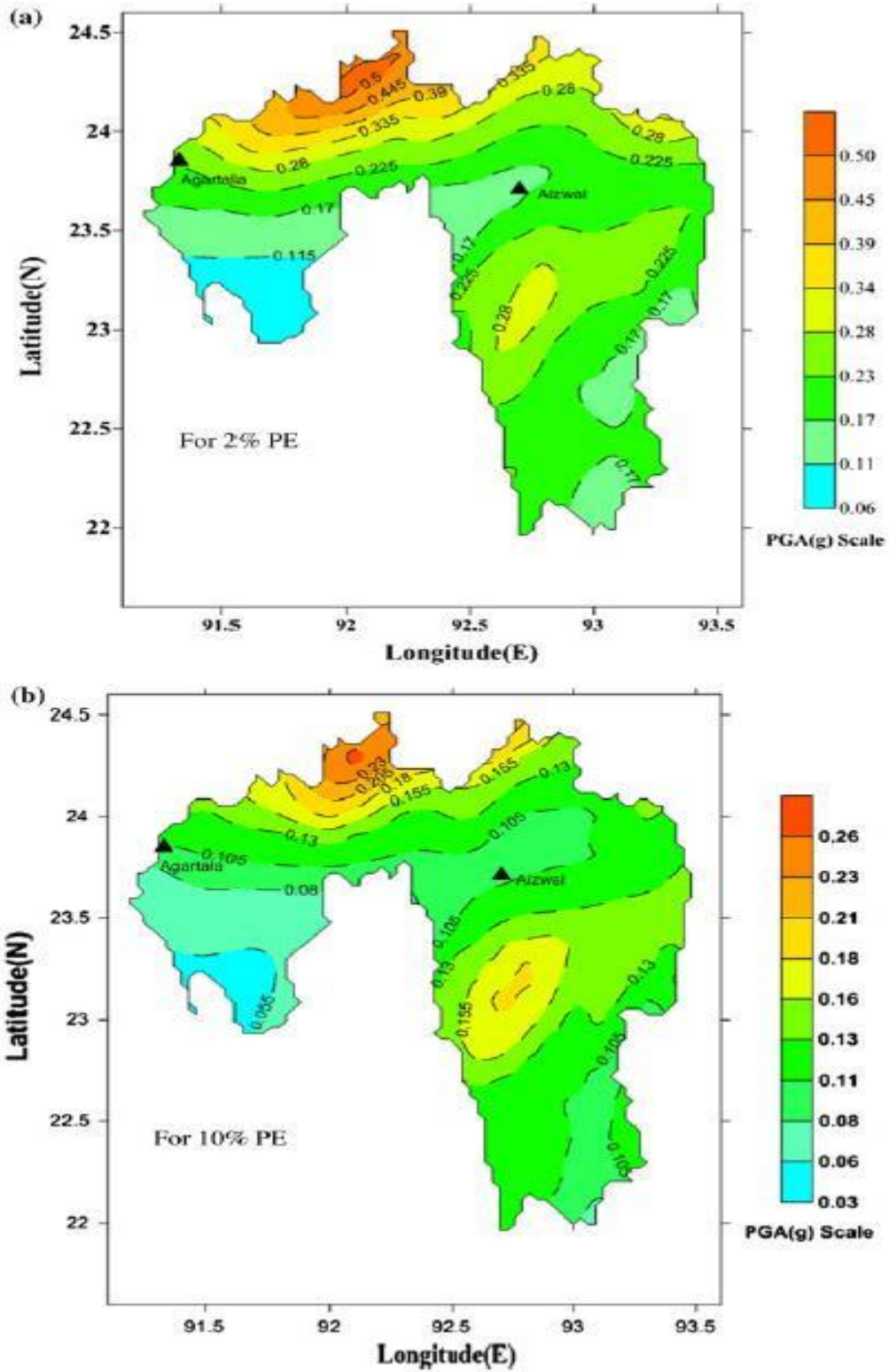


Figure 11 PGA (g) contours at bedrock level for 2 % and 10% likelihood of exceeding in 50 years. (Sil et al., 2013)

The UHS established for Agartala reveals a zero-period spectral acceleration of 0.14 g for a return period of 475 years and 0.20 g for a return period of 2475 years. In the case of Aizawl, these figures are 0.10 g and 0.17 g, respectively. This research utilized two established attenuation models within a logic tree framework and validated them against strong motion data from the region. Unlike the uniform zone factor given for Northeast India in BIS 1893 (2002), this research highlights the spatial variability in seismic hazard across smaller regions of Tripura and Mizoram by considering distinct sources and events at each grid point.

(Das et al., 2016) conducted a seismic hazard assessment (SHA) for the Northeast region of India. The research aims to assess the seismic risk for the area by examining both historical and recorded earthquake data, taking into account various seismic sources, fault characteristics, and seismic patterns. The authors implemented a probabilistic approach to estimate the potential ground shaking levels across different timeframes, underscoring the region's susceptibility to significant seismic occurrences. This study highlights the importance of detailed seismic hazard mapping, which is essential in designing earthquake-resistant buildings and enhancing disaster preparedness in Northeast India. Additionally, this research provides important insights to improve seismic risk management strategies in the region, known for its seismic activity.

The earthquake catalogue for the examined area has been updated and standardized to a single moment magnitude (M_w) scale. This process of homogenization utilized generic orthogonal regression (GOR) algorithms alongside magnitude conversion relationships unique to each site. Furthermore, global GOR relationships were developed using an improved estimation technique, facilitating the conversion of various magnitude types across the entire magnitude spectrum. This method ensured the catalogue's accuracy and consistency, which are visually presented in six figures within the report. Additionally, spectral acceleration (S_a) values for 0.2 and 1-second periods were calculated for exceedance probabilities of 50%, 20%, 10%, 2%, and 0.5% over a span of 50 years. These probabilities correspond to return intervals of roughly 100, 225, 475, 2475, and 10000 years, respectively.

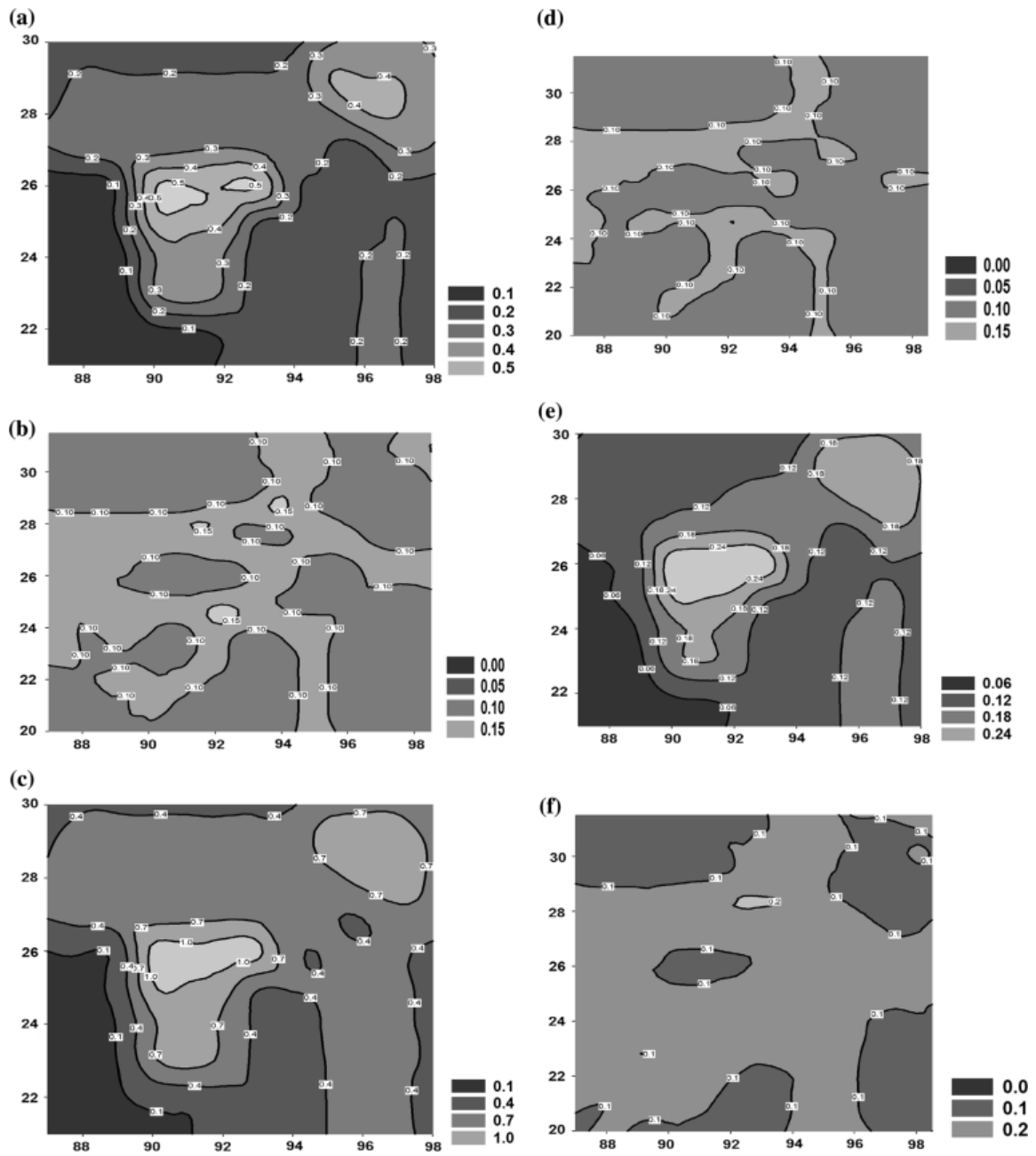


Figure 12 Contour maps of 2% exceedance in 50 years for: a) mean PGA, b) COV for mean PGA, c) Sa at 0.2 s, d) COV for Sa at 0.2, e) Sa at 1.0 s, and f) COV for Sa at 1.0 s. (Das et al., 2016)

The variation in peak ground acceleration (PGA) values across different return periods was examined using a grid-based seismic source model along with ground motion prediction equations (GMPE) provided by Gupta (2010) and Boore & Atkinson (2008). The results, displayed in various figures mentioned in the paper, illustrate the fluctuations of PGA values throughout the study area.

To perform a thorough seismic hazard evaluation for Northeast India, the research region was organized into a grid with a resolution of $0.1^\circ \times 0.1^\circ$. For every grid point, seismic sources within a 300 km radius were assessed to compute PGA and S_a values at the bedrock level. The analysis took into account exceedance probabilities of 50%, 20%, 10%, 2%, and 0.5% over a 50-year time frame. These calculations offered insights into the seismic hazard levels for short (0.2 seconds) and long (1 second) spectral periods, ensuring a thorough comprehension of ground motion behaviour.

The seismic hazard analysis was conducted using CRISIS2007 software (Ordaz et al., 2007), which is a powerful tool for probabilistic seismic hazard assessment. The results, represented in thematic maps, demonstrate the spatial distribution of PGA values for exceedance probabilities of 50%, 20%, 10%, and 2% within a 50-year period. These maps indicate notable differences in seismic hazard throughout the study area, providing essential information for the design of earthquake-resistant structures and risk assessment in the region.

(IS 1893:2016 Part I, 2016) The discussion centres around the Design Basis Earthquake (DBE) and Maximum Considered Earthquake (MCE). Below is a more comprehensive explanation of these concepts and their association with Peak Ground Acceleration (PGA):

The DBE refers to the seismic event that a building is engineered to endure without incurring major damage. It signifies a moderate level of shaking that the structure is expected to withstand during its intended lifespan. This event is related to a 10% likelihood of exceedance over a span of 50 years, typically linked to a recurrence interval of 100 years. It is the benchmark seismic event for structural design.

In the context of seismic hazard evaluation, this means that within a 50-year timeframe, there is a 10% chance that the seismic shaking will meet or surpass the intensity of the DBE.

For design considerations, the PGA associated with the DBE is frequently determined to be 50% of that for the MCE.

The MCE is the most significant seismic event accounted for in the design process, often linked to a very minimal likelihood of occurrence. It corresponds to a 2% probability of exceedance over 50 years. Additionally, it represents the highest level of earthquake shaking that should be factored into the design of buildings in areas prone to high seismic activity.

Relationship Between DBE and MCE:

The Peak Ground Acceleration (PGA) for Maximum Considered Earthquake (MCE) is generally regarded as the highest level of acceleration anticipated from an earthquake occurrence during the designated timeframe. This parameter plays a crucial role in assessing the maximum seismic risk within a specific area. According to the IS

1893:2016 standard, when determining the PGA for Design Basis Earthquake (DBE), it is required to reduce the PGA for MCE by half.

$$PGA_{DBE} = 0.5 * PGA_{MCE}$$

In basic terms, MCE PGA represents the highest level of shaking that the region could face with a 2% likelihood over the next 50 years. On the other hand, DBE PGA indicates a moderate level of shaking that buildings are engineered to withstand, with a 10% probability of being surpassed within 50 years.

PGA Calculation Example:

Table 2 Seismic Zone Factor Z.(IS 1893:2016 Part I, 2016)

Table 3 Seismic Zone Factor Z
(Clause 6.4.2)

Seismic Zone Factor (1)	II (2)	III (3)	IV (4)	V (5)
Z	0.10	0.16	0.24	0.36

For a region in **Seismic Zone V** (according to IS 1893:2016 Table 3):

- The Zonal Factor (Z) for Zone V is **0.36 g**, which represents the PGA for MCE.
- The PGA for DBE would be half of that value:

$$PGA_{DBE} = 0.5 * PGA_{MCE}$$

$$PGA_{DBE} = 0.5 * 0.36$$

$$PGA_{DBE} = \mathbf{0.18\ g}$$

- This means that the PGA for DBE in Zone IV is 0.18 g at bedrock level.

In this instance, the Peak Ground Acceleration (PGA) for Maximum Considered Earthquake (MCE) is 0.36 g, while the PGA for Design Basis Earthquake (DBE) is 0.18 g. This shows that buildings are engineered to withstand moderate shaking during typical situations but are also designed to endure stronger shaking during infrequent events (MCE). The DBE plays a crucial role in ensuring that the structural integrity of buildings is maintained during the most probable earthquakes, minimizing any significant damage. In contrast, the MCE ensures that even the most severe seismic incidents, which are highly unlikely to occur, are taken into consideration, although no substantial structural damage is anticipated in such exceptional circumstances.

(Bahuguna & Sil, 2020) concentrate on assessing the seismic hazards in Assam, calculating the seismicity parameters a and b for various seismic source zones. The characteristics detailed in Table 2 were vital in determining the activity levels within these zones. Out of the 29 identified seismic source zones, 17 were selected for more in-depth analysis based on their a and b values and the highest predicted potential magnitudes. These chosen zones were further examined to develop seismic hazard curves for the 12-district headquarters in Assam, illustrated in Figure 13. These hazard curves, which depict seismic activity at the bedrock level, are crucial for seismic design at both the district and state levels. They can also provide foundational inputs for site-specific studies that take into account faults such as the Main Boundary Thrust (MBT), the Main Central Thrust (MCT), and the Sagging fault.

Table 3 Seismicity parameters of fault/lineaments. (Bahuguna & Sil, 2020)

S.No.	Fault name	Starting		Ending		b -value	a -value	R^2	Active /inactive
		Lat.	Lat.	Long.	Long.				
1	F.2	93.38	20.02	93.67	22.66	0.18	0.22	0.96	Inactive
2	MADHUPUR BLIND FAULT	89.93	24.02	90.14	24.53	0.19	0.18	0.98	Inactive
3	DUDHONI	90.77	25.19	90.8	26.03	0.2	0.24	0.98	Inactive
4	BARAPANI SHEAR ZONE	91.63	25.57	91.98	25.88	0.21	0.19	0.83	Inactive
5	F.3	90.97	26.32	91.84	26.52	0.22	0.29	0.94	Inactive
6	CHEDRANG	90.61	25.82	90.72	26.02	0.23	0.2	0.94	Inactive
7	TISTA	88.67	24.99	89.66	26.77	0.23	0.19	0.89	Inactive
8	F.4	90.33	26.23	90.46	26.53	0.26	0.21	0.98	Inactive
9	A.1	90.24	24.08	90.83	24.9	0.27	0.2	0.85	Inactive
10	PADMA	88.19	24.88	89.74	23.56	0.27	0.15	0.85	Inactive
11	OLDHAM	90.72	25.77	91.73	26.11	0.29	0.25	0.91	Active
12	DAPSI	90.77	25.19	90.8	26.03	0.29	0.16	0.92	Inactive
13	MAT	93.42	23.27	92.99	23.66	0.29	0.22	0.97	Inactive
14	SAMIN	90.53	25.76	90.67	25.9	0.3	0.28	0.97	Active
15	DHUBRI	90	24.6	89.97	26.43	0.38	0.35	0.89	Active
16	LOHITI	95.68	27.71	97.6	28.74	0.4	1.35	0.85	Active
17	DAUKI	92.97	25.12	89.94	25.26	0.47	1.34	0.98	Active
18	DISANG & NAGA THRUST	92.97	25.12	95.06	26.99	0.56	2.32	0.94	Active
19	A.3	93.04	26.31	93.65	26.48	0.58	1.89	0.93	Active
20	SYLHET	90.69	23.99	91.9	24.94	0.61	1.94	0.94	Active
21	KOPILI	91.98	26.92	93.14	25.25	0.63	2.53	0.95	Active
22	MBT & MCT	89.06	27.05	94.33	27.65	0.71	3.36	0.94	Active
23	SAGAING	95.9	20.32	96.62	27.06	0.71	3.43	0.98	Active
24	CMF	93.59	23.96	94.73	26.44	0.71	2.9	0.97	Active
25	MISHMI THRUST	94.35	26.92	97.44	28.9	0.73	3.12	0.97	Active
26	CHITTAGONG COASTAL F.	92.49	20.11	91.39	23.4	0.74	2.57	0.92	Active
27	KALADAN	92.36	20.75	93.09	24.75	0.79	3.52	0.89	Active
28	MYANMAR CENTRAL BASIN	95.52	24.55	95.26	20.38	0.87	4.52	0.94	Active
29	EBT & KABAW	94.17	19.98	96.02	27.07	0.9	4.18	0.97	Active

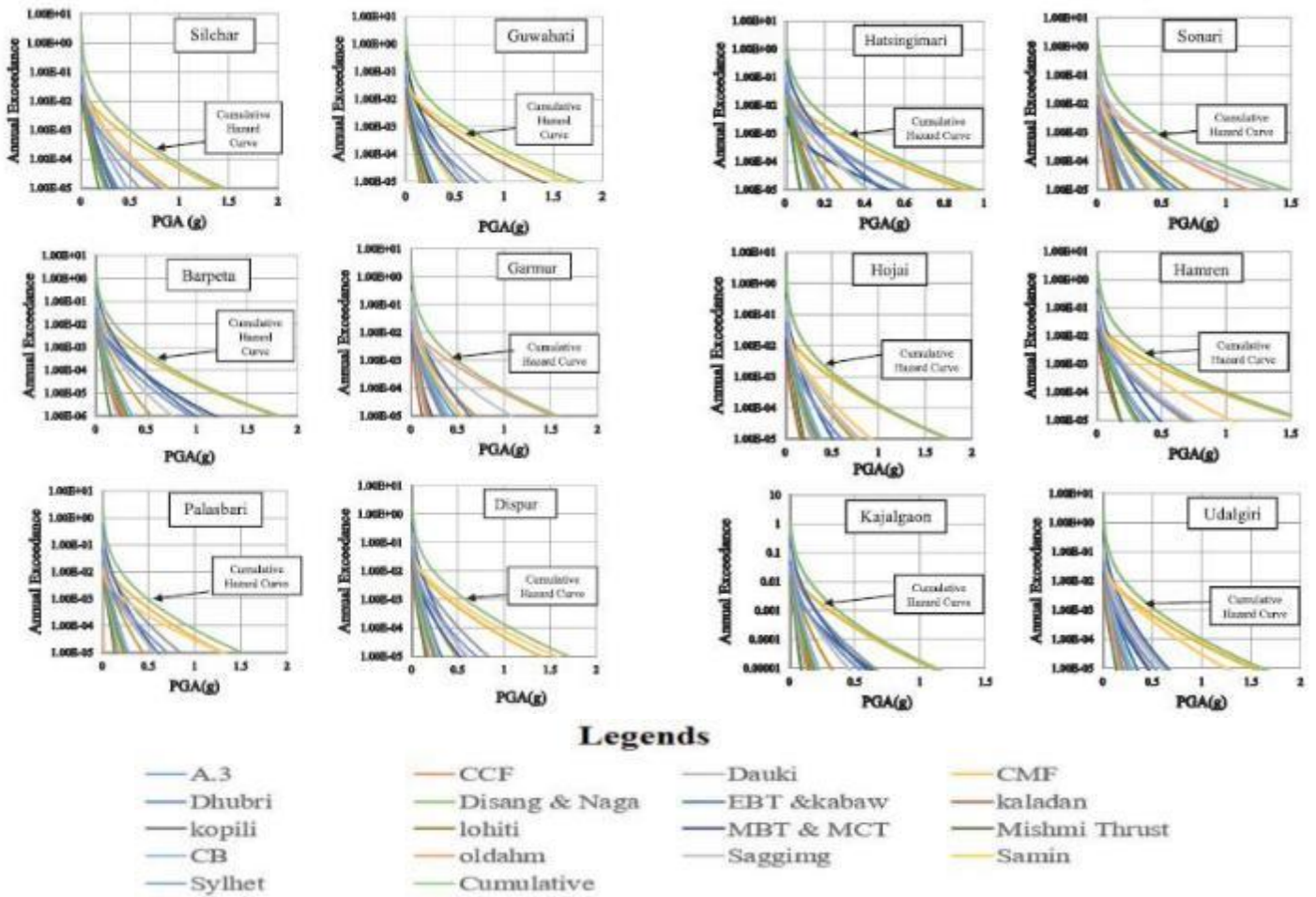


Figure 13 Seismic hazard curve of 12 district headquarters. (Bahuguna & Sil, 2020)

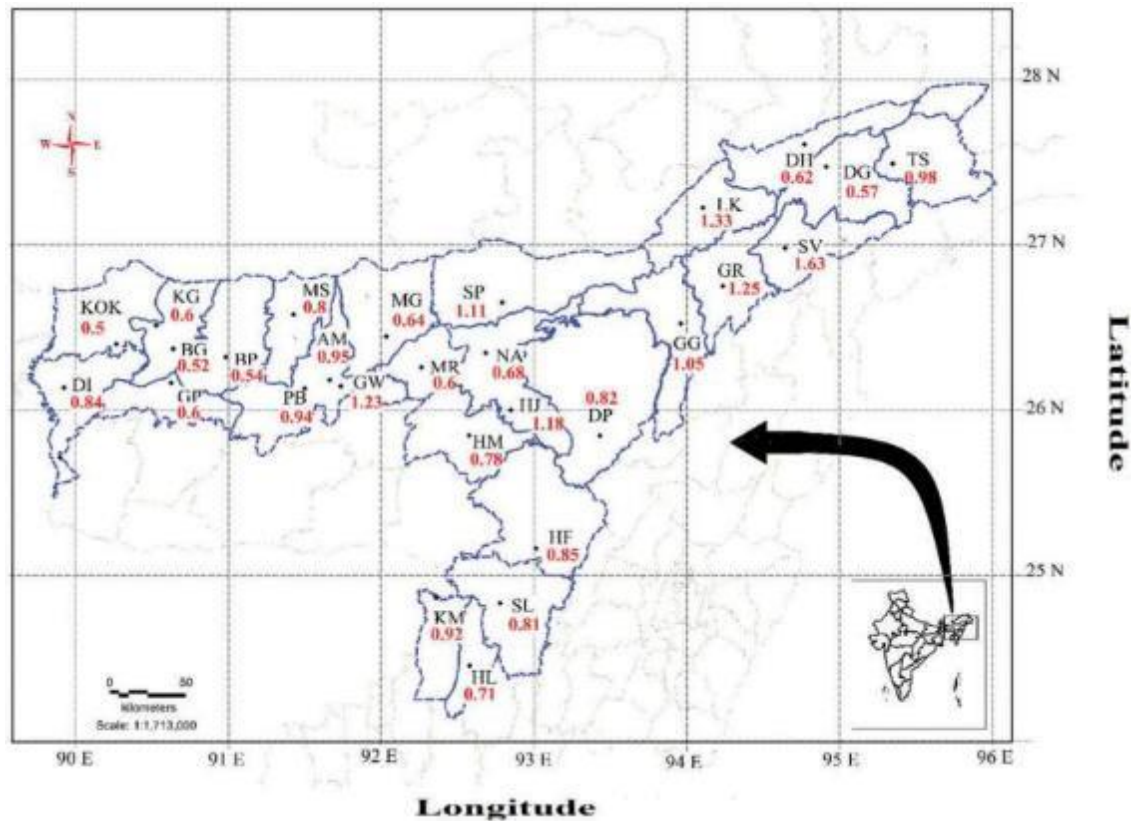
For every district, hazard curves were generated based on distinct fault systems, which were then combined to formulate cumulative hazard curves for the district headquarters at the bedrock level. By employing deterministic seismic hazard analysis (DSHA) and probabilistic seismic hazard analysis (PSHA), the research determined peak ground acceleration (PGA) values for exceedance probabilities of 2%, 5%, and 10% over periods of 50 and 100 years. The findings, illustrated in Table 3 and Figures 14 and 15, indicate that PGA values in Assam range from 0.44 to 0.77 g for a 2% likelihood of exceeding over 50 years and from 0.27 to 0.49 g for a 10% chance within the same timeframe. It is worth noting that several districts exhibit elevated PGA values in the 2% probability scenario, including Guwahati (0.78 g), Tezpur (0.77 g), Mushalpur (0.76

g), and Hojai (0.73 g). For DSHA, PGA values exceeding 1.0 g were observed in districts like North Lakhimpur, Guwahati, and Golaghat.

Table 4 Seismic hazard curve of 12 district headquarters. (Bahuguna & Sil, 2020)

S. no.	City headquarters	DSHA PGA (g)	PSHA PGA (g)					
			2% in 50 years	5% in 50 years	10% in 50 years	2% in 100 years	5% in 100 years	10% in 100 years
1	Barpeta	0.54	0.55	0.42	0.34	0.66	0.51	0.42
2	Bongaigaon	0.52	0.44	0.36	0.35	0.55	0.38	0.36
3	Silchar	0.81	0.64	0.48	0.49	0.78	0.6	0.48
4	Mangaldai	0.64	0.72	0.56	0.48	0.78	0.68	0.56
5	Dhemaji	0.62	0.57	0.45	0.36	0.69	0.56	0.45
6	Dhubri	0.84	0.5	0.37	0.34	0.56	0.45	0.37
7	Dibrugarh	0.57	0.6	0.44	0.35	0.69	0.54	0.44
8	Goalpara	0.60	0.6	0.44	0.34	0.78	0.56	0.44
9	Golaghat	1.05	0.72	0.53	0.41	0.86	0.67	0.53
10	Hailakandi	0.71	0.62	0.49	0.4	0.73	0.58	0.49
11	Diphu	0.82	0.66	0.51	0.43	0.8	0.6	0.51
12	Karimganj	0.92	0.62	0.48	0.39	0.74	0.58	0.48
13	Kokrajhar	0.50	0.51	0.4	0.33	0.59	0.48	0.4
14	North Lakhimpur	1.33	0.71	0.56	0.43	0.85	0.66	0.56
15	Morigaon	0.60	0.63	0.48	0.36	0.78	0.59	0.48
16	Nagaon	0.68	0.6	0.53	0.4	0.66	0.54	0.53
17	Nalbari	0.64	0.58	0.44	0.36	0.7	0.54	0.44
18	Haflong	0.85	0.69	0.52	0.41	0.83	0.65	0.52
19	Sivasagar	1.63	0.62	0.47	0.37	0.75	0.58	0.47
20	Tezpur	1.11	0.77	0.57	0.44	0.94	0.72	0.57
21	Tinsukia	0.98	0.58	0.43	0.34	0.7	0.54	0.43
22	Amingaon	0.95	0.59	0.45	0.35	0.71	0.56	0.45
23	Guwahati	1.23	0.78	0.58	0.46	0.92	0.72	0.58
24	Mushalpur	0.80	0.76	0.57	0.45	0.92	0.72	0.57
25	Udalguri	0.83	0.7	0.53	0.41	0.84	0.66	0.53
26	Kajalgaon	0.60	0.49	0.37	0.3	0.59	0.46	0.37
27	Hamren	0.78	0.7	0.53	0.41	0.84	0.65	0.53
28	Hojai	1.18	0.73	0.55	0.43	0.89	0.69	0.55
29	Sonari	0.70	0.61	0.45	0.36	0.75	0.58	0.45
30	Hatsingimari	0.74	0.43	0.32	0.27	0.52	0.4	0.32
31	Dispur	1.06	0.6	0.42	0.38	0.8	0.5	0.42
32	Palasbari	0.94	0.64	0.48	0.38	0.78	0.6	0.48
33	Garmur	1.25	0.61	0.48	0.37	0.79	0.66	0.48

The variation in PGA values across different regions, illustrated in Figure 14, demonstrates the impact of 17 prominent faults on seismic activity in various districts. The Lohit fault, which has the potential to generate earthquakes up to a magnitude of 9.5, is recognized as a key seismic source for areas such as Barpeta, Mangaldai, North Lakhimpur, and others. Likewise, the Oldham fault, with a maximum potential magnitude of 8.6, serves as the primary source for districts including Silchar,



Hailakandi, and Diphu. For Dibrugarh and Dhemaji, the Sagging fault is noted as the most active, followed closely by the MBT-MCT, EBT, and

Figure 14 The following district headquarters' PGA values were compared using DSHA. (Bahuguna & Sil, 2020)

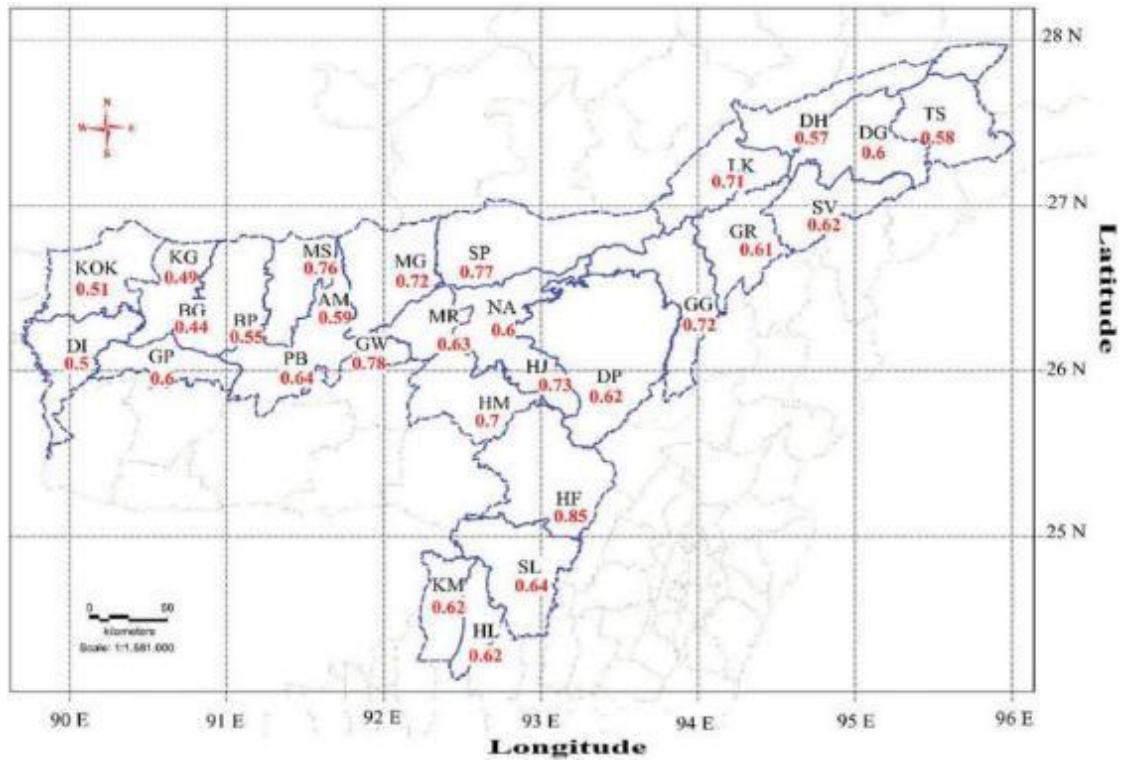


Figure 15 Comparison of the PGA values for district headquarters computed using PSHA for a 2% probability in 50 years. (Bahuguna & Sil, 2020)

the Kabaw fault systems are significant, with the Oldham and Lohit faults primarily responsible for the high PGA values observed in areas like Guwahati, Hojai, and Tezpur. Furthermore, the Sagging fault, which has a maximum magnitude of 8.8, plays a critical role in the seismic activity of certain regions. The seismic hazard assessment utilized data catalogues from various periods, including Parvez et al. (1819–1998), Sharma and Malik (1762–2001), and Sitharam et al. (250 BC–2010). Additionally, strong motion data collected from boreholes in Guwahati was provided by Nath et al. (2009). Identified as a significant seismic source, the Dhubri fault, with a maximum magnitude of 7.5, affects the Dhubri and Hatsingimari districts, relying on data from regions such as Dhemaji, Dibrugarh, and Sonari.

To evaluate seismic risk more effectively in Northeast India and Bhutan, Ghione et al. (2021) introduce a combined probabilistic seismic hazard model that integrates

distributed seismicity with finite fault models. The aim of the research is to enhance the accuracy of seismic hazard forecasts by merging geophysical models with observed seismic data. The hybrid model considers both the regional tectonic framework and particular fault characteristics, including their capacity for generating large-magnitude earthquakes. The study's findings indicate that this method yields a more nuanced and trustworthy assessment of seismic hazards than conventional approaches, underscoring the significance of factoring in both distributed seismicity and active fault zones. These results are vital for the revision of seismic hazard maps and for refining disaster risk management strategies in a region that is exceptionally vulnerable to seismic events.

This research largely depended on the Mw-homogenized ISC-GEM Extended Catalogue as the primary source of earthquake information. However, this catalogue is regarded as complete only for seismic events with magnitudes of 5.0 or higher. To overcome this limitation, future research could incorporate data from local seismological networks, which would enhance the catalogue's completeness, increase the count of recorded seismic occurrences, and enable more thorough statistical analyses. The study also concentrated on declustering the catalogue to accurately model the earthquake generation process as a Poissonian distribution, necessitating the exclusion of aftershocks. The Gardner and Knopoff (1974) technique, originally developed for Southern California, was applied for declustering. Nonetheless, this method removed nearly 40% of the recorded events, resulting in a substantial reduction in the expected seismic activity rates. To mitigate this issue, a manual declustering method was employed, which involves visually identifying and discarding aftershock clusters.

This technique preserved around 75% of the original events for further analysis. Determining completeness periods for various magnitude ranges was another pivotal

element of the study. Findings demonstrated that hazard assessment outcomes were highly sensitive to assumptions regarding completeness, primarily owing to the uneven spatial distribution of seismic activity. To model earthquake occurrences, the study utilized a double-truncated Gutenberg-Richter model. For greater reliability in estimating activity rates, a uniform b-value of 1.05 was applied throughout the study area, allowing the a-value to vary among different sources. The a-values for areal sources were derived from historical seismicity, while those for fault sources were based on slip rate data. Uncertainties in the a-values associated with faults were linked to inaccuracies in GPS measurements and the likelihood that a portion of the slip was realized through plastic deformation. Testing with values spanning from 10% to 80% indicated that a seismic coupling coefficient of 40% was optimal for the area. Future research may explore the impact of reduced slip rates on hazard outcomes. Additional fault characteristics, including geometry, focal mechanisms, and maximum magnitude (M_{\max}), were also examined. M_{\max} for areal sources was calculated by taking the highest measured magnitude and adding 0.5. In contrast, M_{\max} for fault sources was estimated using specific correlations between fault length and magnitude. Preliminary tests modeling entire fault traces produced unreasonably high M_{\max} values. Therefore, segmented fault geometries were created using geological observations, satellite imagery, and historical seismicity distributions. Although fault segmentation models can be subjective, they significantly influence hazard estimation and warrant further investigation in future studies.

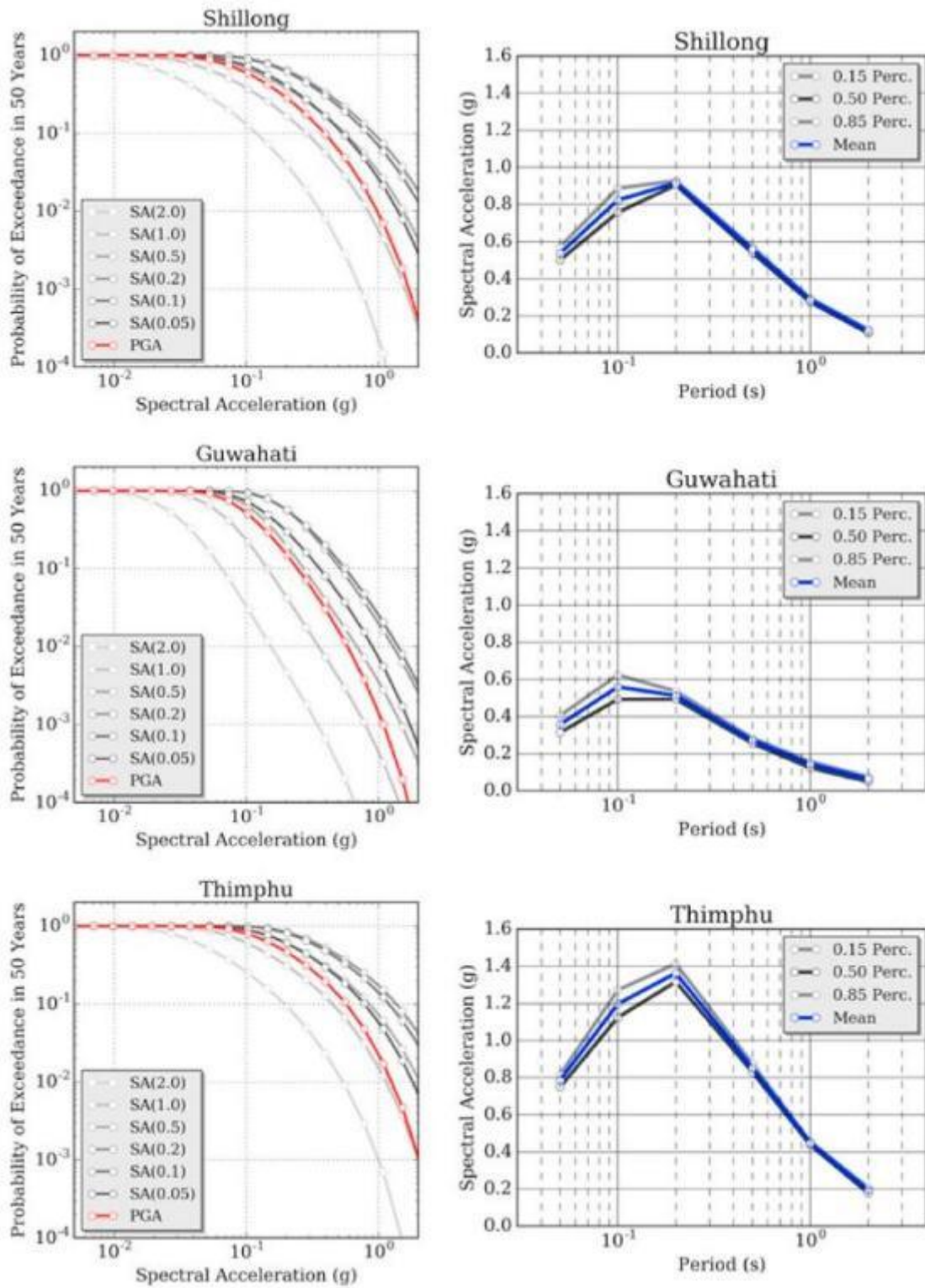


Figure 16 The mean and quantile UHS for various cities at 10% POE in 50 years are on the right, while the mean hazard curves calculated for a variety of spectral periods, including PGA, are on the left. (Bahuguna & Sil, 2020)

Ground Motion Prediction Equations (GMPEs) were essential for this analysis as well. This study evaluated eleven GMPEs that were suitable for both active shallow crust and subduction zones. A logic-tree framework was utilized to incorporate three GMPEs deemed most appropriate for the study area, thereby addressing epistemic uncertainty. However, a significant drawback was the absence of GMPEs specifically calibrated for the local conditions found in Northeast India. Future initiatives could aim at creating GMPEs customized for the Himalayan region, potentially aided by numerical simulations.

One noteworthy finding was the minimal variation in ground motion along the dip direction of thrust faults, which likely resulted from the Joyner-Boore distance metric (R_{jb}) used in the selected GMPEs. While hazard estimates in areal source models were primarily influenced by recurrence rates, the configuration and dip of faults emerged as vital components in fault-based hazard models.

The overall seismic hazard distribution corresponds with the seismic zoning presented in the Indian Building Code (BIS, 2002), which classifies Northeast India as Zone V, representing the highest seismic risk category in the country. This study provides a more detailed assessment of seismic hazards in the area. Due to the influence of the Himalayan décollement and the associated high slip rates, the northern regions of Arunachal Pradesh are identified as having greater seismic hazards compared to Assam and Meghalaya. In Assam and Meghalaya, significant increases in hazard levels were noted when active faults were included in the analysis.

(Bandyopadhyay *et al.*, 2022) used a detailed earthquake catalogue that spans from 1735 to 2021 to perform a Probabilistic Seismic Hazard Analysis (PSHA) for the northeastern region of India. The study area displays a variety of tectonic conditions, including active continental crust, subduction zones, and shallow intraplate crust of India. To accommodate these differences, eight specific Ground Motion Prediction Equations (GMPEs) that are suited to the regional seismic characteristics were utilized. The uncertainties involved in seismic hazard evaluation were addressed using a logic-tree methodology. As part of the study, hazard maps were produced, and uniform hazard spectra (UHS) were obtained for six cities in Assam, considering return periods (RPs) of 475, 2,475, 975, and 9,975 years. Moreover, a soil enhancement investigation was carried out for the Guwahati region using borehole data from five representative sites throughout the city, facilitating the creation of surface-level spectra. Key findings from the study are summarized as follows:

- Peak Ground Acceleration (PGA) for Guwahati Region:

The PGA values corresponding to return periods of 475, 975, 2,475, and 9,975 years were determined to be 0.25 g, 0.32 g, 0.42 g, and 0.63 g, respectively, at the bedrock level. The increase in bedrock UHS was identified as being between 2.3 and 2.5 times the PG. The spectral peak was observed in the high-frequency range of 0.07 to 0.1 seconds (10-15 Hz). The PGA findings for the 475- and 2,475-year return periods align with previous research.

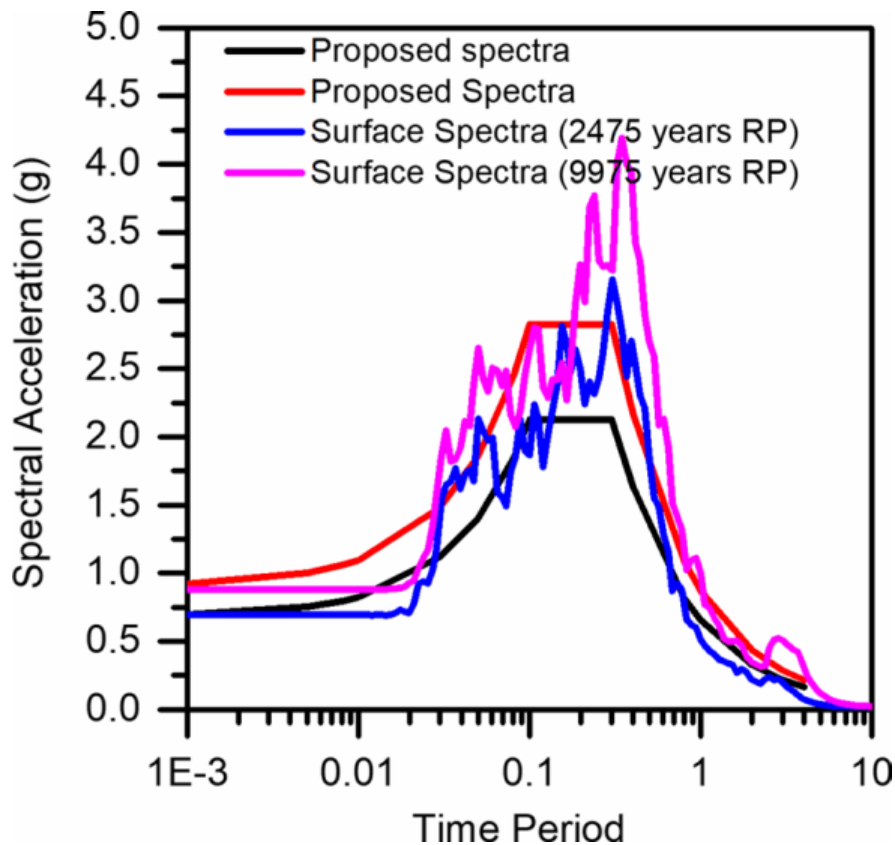


Fig. 17 Guwahati city’s ground level spectra (5% damped) for over 2500 years and 10,000 years, respectively . (Bandyopadhyay et al., 2022)

- Peak Ground Acceleration (PGA) for the Himalayan Region: For the Himalayan area, recognized as India's most seismically active zone, the bedrock-level PGA for a 2,475-year time period was calculated to be 0.59 g. This indicates that seismic accelerations at the bedrock level in these high-seismicity regions may be further amplified by soil effects, highlighting the need for comprehensive regional investigations.
- UHS for Cities in Assam: Among the six cities examined, Guwahati and Tezpur demonstrated the highest peak ground acceleration (PGA) values at rock outcrops for a return period of 9,975 years, with measurements of 0.63 g and spectral peaks of 1.47 g and 1.39 g, respectively. In contrast, Dibrugarh and Jorhat recorded lower PGA values of 0.54 g, while their spectral peaks reached

1.33 g. These rock-level spectral data are essential for designing structures directly on rocky surfaces or for calculating surface-level spectra for sites with soil.

- **Soil Amplification in Guwahati:** Soil amplification studies revealed that for Guwahati, the PGA increased to 0.696 g for a 2,475-year RP and 0.924 g for a 9,975-year RP. These results highlight substantial amplification effect caused by the alluvial soil prevalent in the region. Critical infrastructure in these areas should be developed using area-specific surface-level seismic spectra to ensure safety along with conservatism.
- **Amplification and Frequency Shifts:** The surface-level spectra for Guwahati, with 5% damping, showed a peak amplification of 3.12 times the PGA for both the 2,475- and 9,975-year RPs. This amplification occurred within the frequency range of 3–10 Hz. Notably, soil amplification shifted the spectral peaks from the higher frequency range of 10–15 Hz at the bedrock level to a lower frequency range of 3–5 Hz. This emphasizes the need for designers to account for such shifts when designing structures on soft alluvial soils.

These findings underscore the critical importance of incorporating site-specific soil conditions into seismic hazard assessments and provide a robust framework for designing earthquake-resistant structures in the northeastern region of India.

3.2 Summary of the Literature Review

Table 5 The PGA value contrasts with other research for the PSHA approach (10% in 50 years).

(For an exact comparison, Guwahati city was picked from all research.)

Authors	PGA
Sharma and Malik (2006)	0.50g
Nath et al. (2012)	0.66g
Sil et al. (2013)	0.36g
Das et al. (2016)	0.24g
IS-1893 (2016)	0.18g
Bahuguna and Sil (2020)	0.46g
Bandyopadhyay et al., (2022)	0.25g

Table 5 presents various PGA values reported by different researchers. The differences in these results can be attributed to the selection of distinct attenuation models and the fluctuation in seismicity parameters arising from changes in the earthquake catalogue. Therefore, these findings underscore the significance of obtaining the most current PGA value for the specific location where we intend to conduct further analysis on any infrastructure.

3.3 Identified Research Gaps

Although numerous studies have evaluated seismic hazards at regional or national scales, there is a significant gap in detailed assessments aimed at particular locations. A majority of current research fails to account for local elements such as soil composition, terrain features, and distance from fault lines, all of which can significantly affect ground shaking during seismic events. Key seismic indicators like Peak Ground

Acceleration (PGA), Peak Ground Velocity (PGV), and Spectral Acceleration (SA) differ across various locations, and relying on generalized models may not accurately represent the specific risk at an individual site. In the absence of localized studies, design approaches may lack reliability, resulting in structural vulnerabilities and inadequate disaster preparedness. This underscores the necessity for targeted seismic hazard evaluations that take into account local geological and seismological factors, essential for ensuring safer infrastructure planning and building practices.

3.4 Justification for Site-Specific Seismic Hazard Assessment

Due to the significance of precise ground motion estimation in designing and ensuring the safety of critical infrastructure, this study focuses on a practical case: the planned construction of a new bridge at Saraighat located in Guwahati, Assam. This area is within a seismically active zone and is affected by nearby active faults, which makes it vital to assess the seismic hazard at the site before proceeding with detailed structural design. As a result, conducting a site-specific seismic hazard assessment—utilizing both deterministic and probabilistic methods is essential to supply dependable input parameters such as Peak Ground Acceleration (PGA) and spectral acceleration values needed for the seismic design of the Saraighat Bridge.

CHAPTER 3

METHODOLOGY FOR CASE STUDY

This chapter outlines the comprehensive method used to perform a site-specific seismic hazard assessment (SSSHA) for the planned Saraighat Bridge. The approach incorporates both Deterministic Seismic Hazard Analysis (DSHA) and Probabilistic Seismic Hazard Assessment (PSHA) to provide an in-depth understanding of the seismic risks associated with the bridge site. The process involves collecting data, characterizing seismic sources, selecting ground motion prediction models, and estimating hazards through established computational tools and techniques.

4.1 Introduction for Case Study

The Saraighat Bridge crosses the Brahmaputra River in Assam and plays a crucial role in the transportation system of Northeast India, accommodating both road and rail traffic. Due to its vital role in facilitating regional and national connectivity, it is necessary to perform a thorough assessment of the seismic hazards present at this location. Assam and a large portion of Northeast India fall under Seismic Zone V as per IS 1893:2016, which signifies the highest level of seismic risk in India. This designation is founded on the region's past experiences with major earthquakes, primarily caused by the ongoing collision between the Indian and Eurasian tectonic plates.

The area has a history of several significant earthquakes, including the 1897 Shillong earthquake (Mw 8.1) and the 1950 Assam–Tibet earthquake (Mw 8.6). These notable events underscore the insufficiency of depending solely on general regional seismic mapping, which does not account for localized geological features and specific fault

characteristics. Thus, a tailored hazard assessment at the site is crucial for a more comprehensive understanding of ground motion behaviour at the structural level. This research performs a detailed seismic hazard analysis for the Saraighat Bridge location through both Deterministic Seismic Hazard Analysis (DSHA) and Probabilistic Seismic Hazard Assessment (PSHA). The DSHA approach seeks to estimate the maximum ground motion for the site by considering the most extreme earthquake scenario and proximity to the nearest fault, while PSHA evaluates a range of potential earthquakes, accounting for uncertainties in magnitude, recurrence, and distance to provide estimates for ground motion across various return periods, such as 475 and 2,475 years.

To execute the assessment, earthquake catalogue data from multiple sources is collected and analysed. This information undergoes conversion for magnitude, declustering to remove dependent events, and completeness checking. Seismic source zones are defined, and essential seismic parameters, such as Gutenberg–Richter a and b values along with maximum magnitude estimates, are evaluated for each fault. Appropriate Ground Motion Prediction Equations (GMPEs) that match the area's tectonic conditions are used to calculate site-specific Peak Ground Acceleration (PGA). Hazard curves and Uniform Hazard Spectra (UHS) are generated to determine seismic input values for design considerations. The outcomes of this study are expected to greatly improve both scholarly knowledge and practical applications. The results will assist engineers, planners, and government entities in understanding seismic risks, guiding retrofitting projects, and enhancing the overall resilience of vital transportation infrastructure in the region.

4.2 Data Collection

The seismic data used in this study consists of:

- **Historical earthquake catalogues**, compiled from sources such as the United States Geological Survey (USGS) and the Indian Meteorological Department (IMD), covering the period from 1763 to the present.
- **Fault and tectonic data**, including the locations and characteristics of nearby active faults such as the Kopili Fault, Dauki Fault, Main Boundary Thrust (MBT), and others.

The initial earthquake catalogue consisted of magnitudes reported in various scales, including surface wave magnitude (M_s), body wave magnitude (M_b), and local magnitude (M_L). To maintain consistency and ensure suitability for seismic hazard analysis, it was necessary to convert all values to moment magnitude (M_w), which is the standard metric for such studies.

The process of magnitude homogenization was carried out using empirical relationships developed by (Sitharam & Sil, 2014) specifically tailored for the seismic characteristics of Northeast India. The conversion formulas used were:

$$M_w = 0.862 \times M_b + 1.034$$

$$M_w = 0.673 \times M_L + 1.730$$

$$M_w = 0.625 \times M_s + 2.350$$

Equation 1 Empirical relationship developed by Sitharam & Sil, 2014.

By applying these relationships, the final catalogue was standardized to a consistent magnitude scale. This uniformity minimizes systematic discrepancies and enhances the

reliability of recurrence rate calculations required for both deterministic and probabilistic seismic hazard analyses.

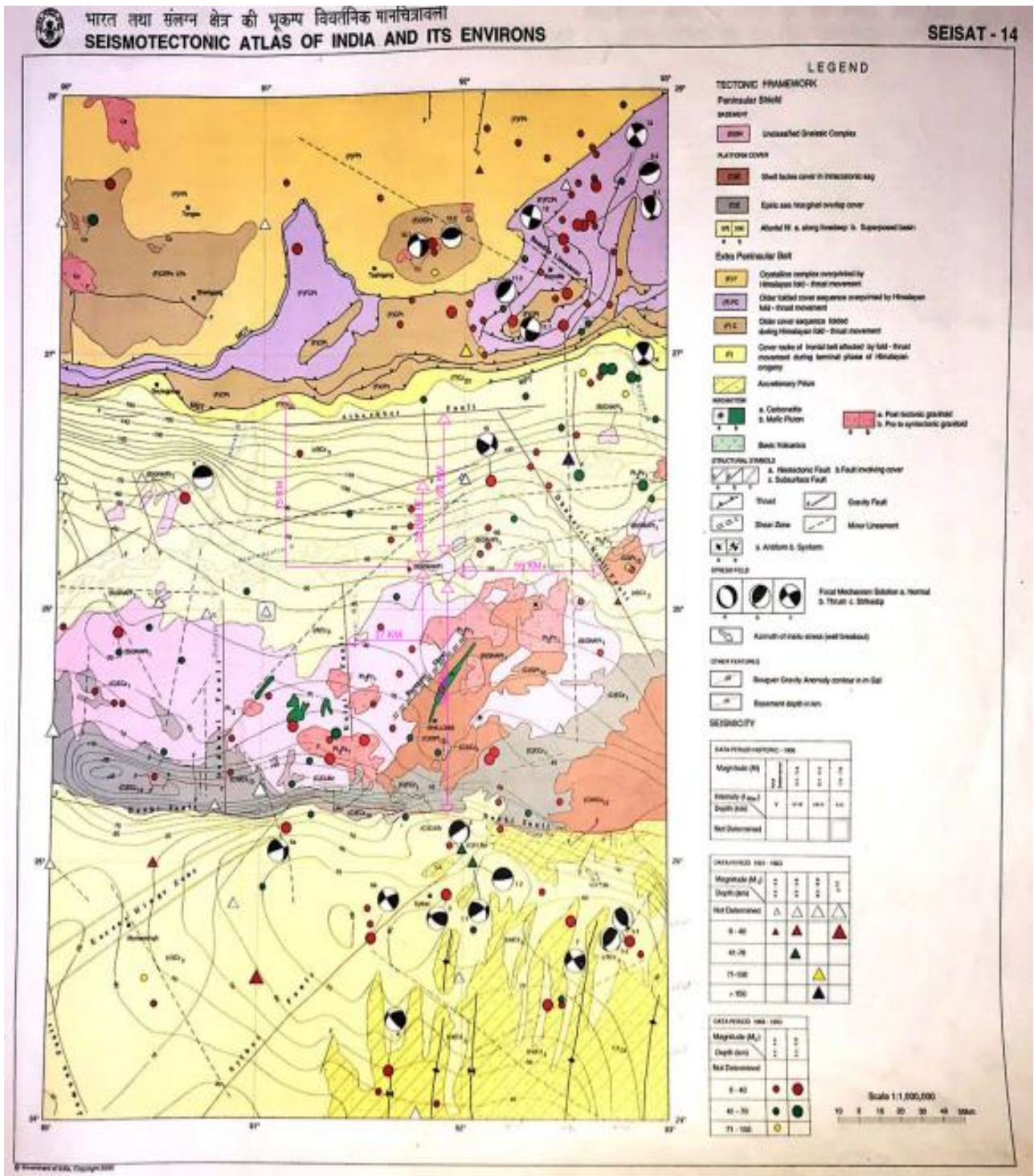


Figure 17 Faults and their distance from Saraighat Bridge.

4.3 Declustering of Earthquake Catalogue

Earthquake catalogues frequently include related events such as aftershocks and foreshocks, which can artificially elevate seismicity rates and skew hazard assessments. To mitigate this issue, the catalogue was declustered utilizing the space-time windowing method proposed by Gardner and Knopoff (1974), a technique widely recognized in seismic research. This method eliminates clustered events while keeping only statistically independent mainshocks, which are crucial for accurately determining recurrence rates in both deterministic and probabilistic hazard evaluations.

4.4 Completeness Analysis

A crucial aspect of reliable seismic hazard evaluation is confirming that the earthquake catalogue is thorough for the considered magnitude ranges. Completeness indicates that, within a specific time frame, all earthquakes above a designated magnitude threshold have been consistently recorded. To determine these durations for the Saraighat Bridge area, the Cumulative Number versus Time (CUVI) method was utilized.

Initially, the homogenized and declustered catalogue was segmented into four standard magnitude ranges: M_w 4.0 – 4.9, M_w 5.0 – 5.9, M_w 6.0 – 6.9, and $M_w \geq 7.0$. For each magnitude range, a plot was created illustrating the cumulative number of earthquakes over time. The trend observed offers a distinct visual representation of data reliability. A linear and consistently increasing segment indicates that events have been reliably

recorded during that timeframe. Conversely, a flat or irregular segment implies underreporting or missing data.

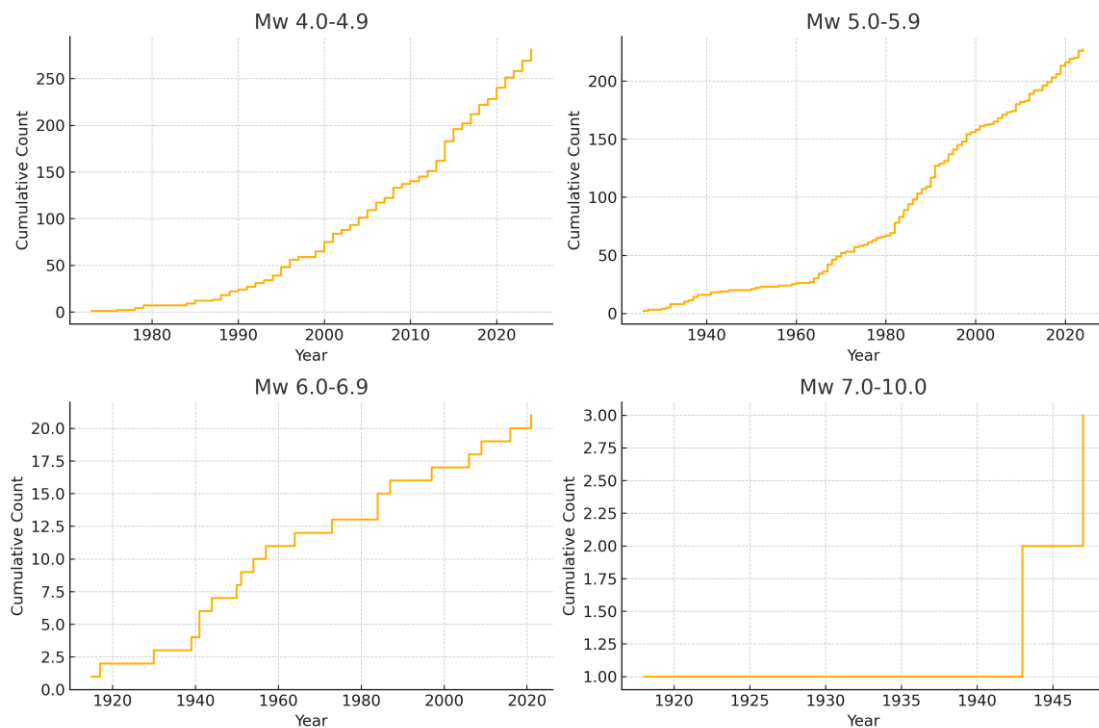


Figure 18 Plot of Data Completeness by CUVI method.

Through the examination of these plots, the initial year for dependable records within each magnitude category was identified as the point where the slope becomes stable and linear, continuing without notable interruptions. In the Saraighat dataset, this led to the following completeness periods:

Mw 4.0–4.9: complete from 1976 onward

Mw 5.0–5.9: complete from 1931 onward

Mw 6.0–6.9: complete from 1939 onward

Mw \geq 7.0: complete from 1918 onward

Only earthquakes occurring within these periods were considered for calculating Gutenberg–Richter recurrence parameters. Implementing completeness in this manner ensures that seismicity rates and hazard assessments do not undervalue due to absent or sparse early data. The method based on CUVI is widely recognized in seismic hazard research because it provides an open, justifiable approach for establishing data reliability thresholds.

Mw Range	Completeness Year
4.0–4.9	1976
5.0–5.9	1931
6.0–6.9	1939
≥ 7.0	1918

4.5 Seismic Source Characterization

A crucial element of seismic hazard assessment involves identifying and detailing seismic sources like faults, fault zones, or larger seismogenic regions, that could potentially cause earthquakes impacting the site. In this analysis, the selection of sources was determined based on multiple factors, such as tectonic relevance, historical earthquake activity, closeness to the Saraighat Bridge site, and corroborating data from earlier seismotectonic studies.

Selection of Source Zones

Following a detailed review of regional geological and seismic studies, six primary fault sources were chosen for the site-specific analysis:

- Oldham Fault
- Samin Fault
- Kopili Fault
- Dauki Fault
- A3 Fault
- Main Boundary Thrust (MBT)

These faults were selected because they:

1. Fall within the defined region of interest (**24°–28.5°N, 89°–94.5°E**)
2. Exhibit a record of past seismic activity supported by both instrumental and historical data
3. Represent prominent active faults or thrust zones within the tectonic framework of Northeast India

Although other regional faults, such as the Lohit Fault and Mishmi Thrust, have been included in broader hazard models, this study focuses on the most relevant sources near the bridge location to ensure a targeted, site-specific hazard assessment.

Table 6 Details of various faults considered in the study.

Fault	Starting Long.	Starting Lat.	Ending Long.	Ending Lat.	Length (km)	Depth (km)
Samini F.	90.53	25.76	90.67	25.9	20	26
Dauki F.	92.97	25.12	89.94	25.26	320	54
Oldham F.	90.72	25.77	91.73	26.11	110	31
A3 F.	93.04	26.31	93.65	26.48	80	38

Kopili F.	92.5	26.0	93.5	27.5	300	32
MBT	93.0	91.50	28.30	27.50	200	45

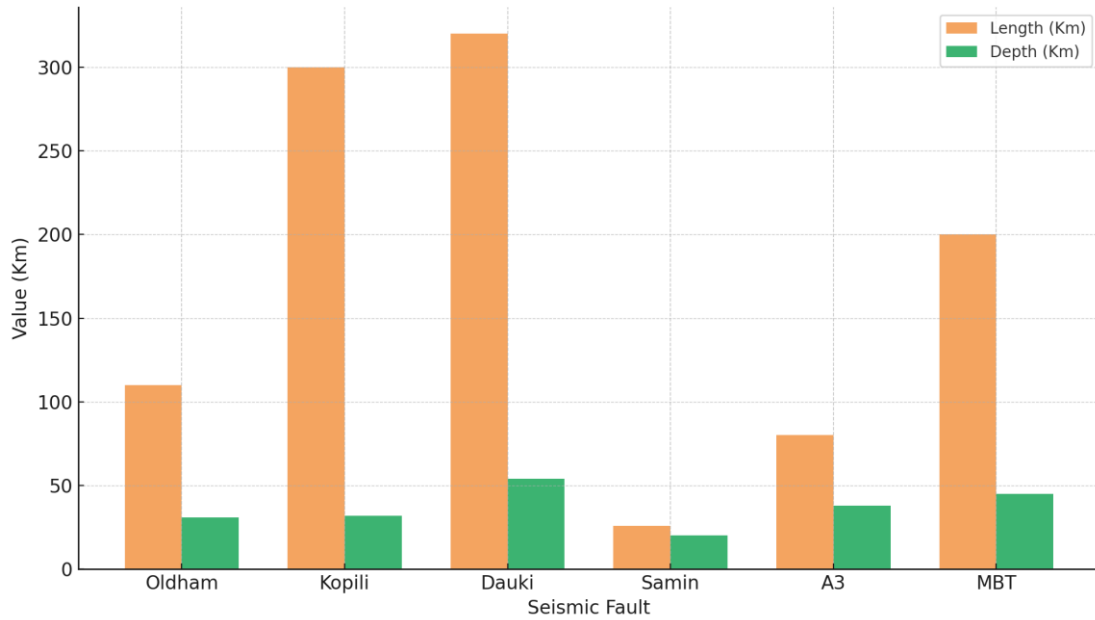


Figure 19 Comparison of Length and Depth of Considered Seismic Sources.

Relevance of Selected Seismic Sources

Each fault selected for this study represents a unique tectonic setting relevant to the regional seismic behaviour:

- The **Oldham** and **Kopili Faults** are strike-slip structures located within the Shillong Plateau.
- The **Samín** and **A3 Faults** are identified as active crustal faults.
- The **Dauki Fault** serves as the boundary between the Shillong Plateau and the Bengal Basin.

- The **Main Boundary Thrust (MBT)** is a major thrust fault marking the Himalayan frontal zone.

By incorporating these diverse source types, the analysis captures both local (near-field) and broader regional influences, ensuring a comprehensive seismic hazard assessment for the Saraighat Bridge site.

4.6 Assigning Earthquakes to each faults

In the research conducted by (Mishra et al., 2024) segments of faults are characterized using geographic coordinates for their starting and ending points. The midpoint of each fault is calculated through computational methods based on these endpoints. For each earthquake recorded in the declustered seismic catalogue, the geodesic distance (measured in kilometres) between the event's epicentre and the midpoint of each fault is computed. Earthquakes are classified with a specific fault if they occur within a radius of 50 km from its midpoint. Rationale for the 50 km Radius This distance criterion is commonly utilized in seismic hazard evaluations because of its empirical and theoretical significance. Notable studies that support this methodology include:

(Nath & Thingbaijam, 2012)

(Bahuguna & Sil, 2020)

(*Sil et al., 2013*)

This approach guarantees a systematic association between faults and events, while aligning with established standards in seismotectonic studies.

Fault	Events Assigned
--------------	------------------------

A3	57
Dauki	75
Kopili	84
MBT	100
Oldham	61

4.7 Computation of seismic parameters

An essential component of both deterministic and probabilistic seismic hazard analysis is the estimation of seismicity parameters that describe the frequency-magnitude relationship of earthquakes within each seismic source zone. These parameters are derived from the Gutenberg-Richter recurrence law, which statistically describes the expected number of earthquakes exceeding a given magnitude over a specified time and area.

Gutenberg-Richter Relationship

The Gutenberg-Richter (G-R) law is expressed as:

$$\log_{10}N(M) = a - bM$$

Equation 2 Gutenberg-Richter (G-R) law.(Beitr, n.d.)

where:

- $N(M)$ is the cumulative number of earthquakes with magnitude $\geq M$,
- a is the activity rate, reflecting the overall seismicity level,
- b is the slope, reflecting the relative proportion of small to large events.

To calculate these parameters, the prepared and declustered earthquake catalogue (M_w homogenized) was analysed for each defined seismic source zone.

Estimation of a-Value and b-Value

For each fault:

1. The earthquake magnitudes were rounded to 0.1 or 0.2 Mw bins.
2. The cumulative frequency distribution $N(M)$ was computed.
3. The $\log_{10}N(M)$ vs. M plot was created, and a linear regression was applied to the linear portion of the curve.
4. The slope of the line gave the $-b$ -value, and the intercept gave the a -value.

These calculations were performed individually for:

- Oldham Fault
- Samin Fault
- Kopili Fault
- Dauki Fault
- A3 Fault
- Main Boundary Thrust (MBT)

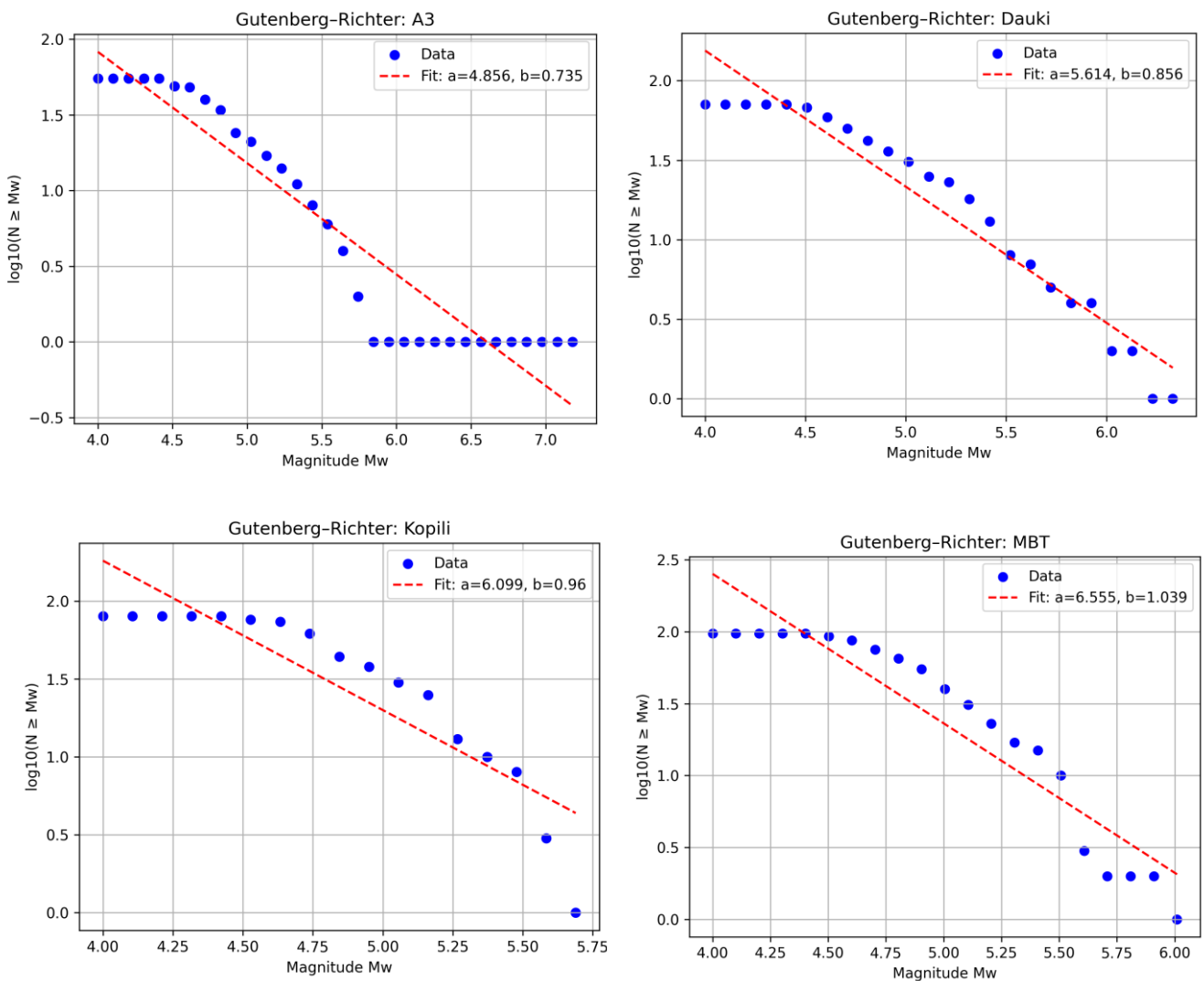
Initially, only earthquakes identified within a 50 km buffer zone for each fault and filtered according to their completeness year were taken into account. The declustered, uniform magnitudes (M_w) were categorized into intervals (typically 0.1 or 0.2 Mw increments). For every bin, the total number of earthquakes with magnitudes equal to or exceeding the lower limit of the bin was calculated.

A chart was subsequently created with magnitude displayed on the x-axis and the base-10 logarithm of the cumulative count of events on the y-axis. A least squares regression

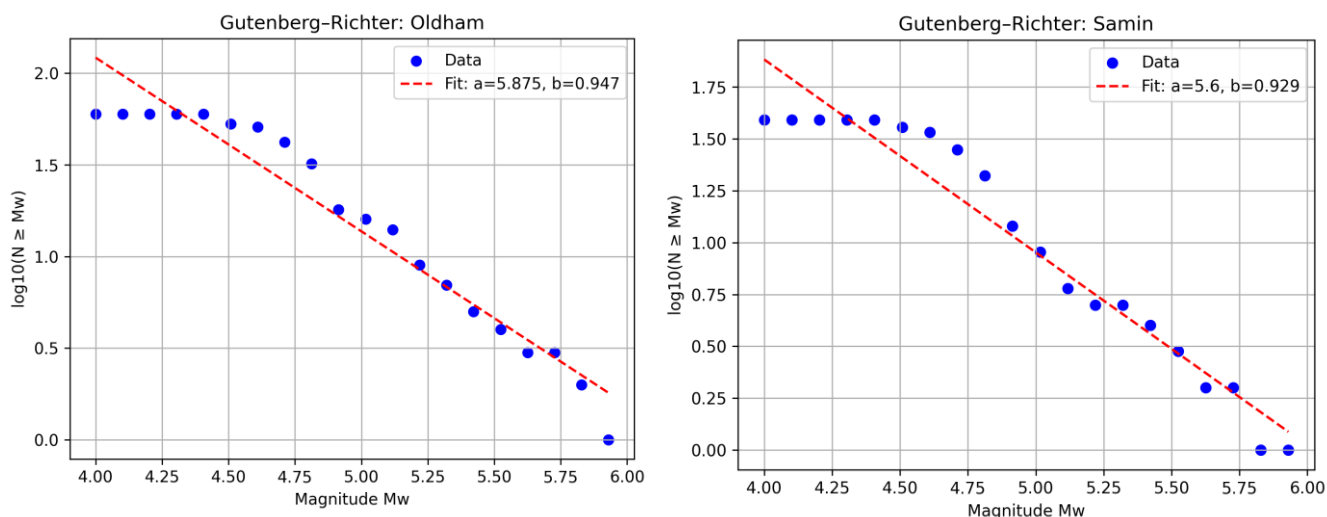
analysis was conducted to fit a straight line to these data points. The y-intercept of this line determines the a-value, while the negative slope yields the b-value for that particular fault.

By deriving a- and b-values for each fault separately, the model accounts for differences in seismicity throughout the area. This fault-specific methodology enhances the accuracy of hazard assessments compared to utilizing a singular regional value.

Table 7 Calculated a & b Value.



Fault	a	b	No of events
-------	---	---	--------------



Dauki	5.614	0.856	71
Samin	5.6	0.929	39
Oldham	5.875	0.947	60
A3	4.856	0.735	55
Kopili	6.099	0.96	80
MBT	6.555	1.039	97

Figure 20 G - R Plots for each fault.

4.8 Estimation of Maximum Magnitude (M_{max})

To establish the maximum credible magnitude (M_{max}) for each fault zone, this study utilized both historical data and statistical methodologies. The approach is aligned with the methods outlined by (Kijko & Graham, 1998) and (Kijko, 2004) which involves statistically adjusting the largest recorded earthquake to reflect the limitations of

observation duration. Specifically, the adjustment formula incorporates 0.5 divided by the fault's b-value and adds this to the largest observed magnitude. This straightforward technique is often referenced in seismic hazard literature as an effective means to account for the possibility that larger earthquakes have yet to be recorded in contemporary history. Furthermore, (Kumar Jaiswal et al., 2002) advise including a constant of 0.5 M_w as a conservative adjustment. By evaluating both estimates, the larger figure is chosen as the fault's M_{max} . This approach yields a justifiable maximum magnitude input that integrates available empirical data with a recognized statistical correction.

Table 8 Estimation of Mmax Values.

Fault	Max Observed M_w	b-value	Mmax Jaiswal	Mmax Kijko	Final Mmax
Dauki	6.92	0.85	7.42	7.51	7.51
Samin	6.96	0.93	7.46	7.5	7.5
Oldham	5.93	0.95	6.43	6.46	6.46
A3	7.18	0.75	7.68	7.85	7.85
Kopili	5.69	0.96	6.19	6.21	6.21
MBT	6.01	1.03	6.51	6.5	6.51

Final Parameters Table

The final set of seismicity parameters used for the hazard assessment such as fault length, minimum distance, M_{max} , and Gutenberg–Richter a- and b-values—were compiled into a summary table to support ground motion modeling.

Table 9 M_{max} and M_{min} values of faults.

Fault Name	a-value	b-value	M_{max}	M_{min}
Dauki	5.614	0.85	7.51	4.5
Samin	5.6	0.93	7.5	4.5
Oldham	5.875	0.95	6.46	4.5
A3	4.856	0.75	7.85	4.5
Kopili	6.099	0.96	6.21	4.5
MBT	6.555	1.03	6.51	4.5

Accurate estimation of seismicity parameters ensured that both deterministic and probabilistic analyses were grounded in statistically reliable recurrence models, thereby enhancing the credibility of the resulting seismic hazard estimates.

4.9 Ground Motion Prediction Equations (GMPEs)

Ground motion prediction equations (GMPEs) play a crucial role in evaluating seismic hazards by offering empirical correlations that allow for the estimation of ground motion parameters, including Peak Ground Acceleration (PGA) and Spectral Acceleration (S_a), based on factors such as earthquake magnitude, distance from the source, and site characteristics. In this research, GMPEs were employed to transform seismic source information into ground motion predictions tailored to the specific location of the Saraighat Bridge.

Selected GMPE Models

Two models were selected to capture both national and regional seismic behavior:

1. NDMA (2011) GMPE

- Developed for Indian conditions under the National Seismic Hazard Mapping Project.
- Suitable for rock site conditions.
- Equation:

$$\log_{10}(PGA) = -1.962 + 0.953M - 1.21 \cdot \log_{10}(R+25)$$

Equation 3 NDMA (2011) GMPE

Where M is moment magnitude and R is hypocentral distance (in km).

2. Bajaj & Anbazhagan (2019) GMPE

- Developed using strong motion data from Northeast India.
- Calibrated for both rock and soil conditions.
- Equation:

$$\log_{10}(PGA) = -3.512 + 1.065M - 1.255 \cdot \log_{10}(R + 20)$$

Equation 4 Bajaj & Anbazhagan (2019) GMPE

Where M is moment magnitude and R is epicentral distance (in km).

These two models were chosen to ensure representation of both national standards and regional ground motion characteristics.

Averaging and Site Amplification

To generate representative site-level ground motion estimates:

- Equal weights (50% each) were applied to the PGA values predicted by both GMPEs.
- In the DSHA, a soil amplification factor of 1.3, which does not depend on the time period, was used on the determined bedrock PGA. This modification considers the local Site Class D soil conditions commonly found in Guwahati alluvium, adhering to the guidelines of IS 1893 (2016) and regional site response research. The amplified figure reflects the anticipated surface-level shaking that the structure will truly encounter.

Application in DSHA and PSHA

- In **DSHA**, the GMPEs were used with each fault's maximum magnitude (M_{max}) and minimum distance (R_{min}) to compute deterministic PGA values.
- In **PSHA**, the models were integrated over a range of magnitudes and distances, incorporating probability distributions and uncertainty (σ) to calculate probabilistic ground motion levels.

This combined approach allowed for accurate, site-specific ground motion estimates, supporting the development of hazard curves and design-level seismic inputs.

4.10 Deterministic Seismic Hazard Assessment (DSHA)

Deterministic Seismic Hazard Assessment (DSHA) offers a cautious assessment of the highest expected ground motion at a location by analysing the most significant plausible earthquake on the closest or most dangerous fault. In contrast to probabilistic approaches, DSHA does not incorporate the probability of occurrence over time but rather emphasizes extreme scenarios, which are especially important for essential infrastructure where the repercussions of failure can be severe.

Results

Table 10 Values of PGA for each fault at bedrock

Fault	Mmax	Distance (km)	PGA_NDMA (g)	PGA_Bajaj (g)	Final DSHA PGA (g)
Oldham	6.46	10.73	0.876	0.394	0.635
A3	7.85	135.3	0.536	0.227	0.381
Dauki	7.51	112.9	0.465	0.192	0.328
Samin	7.5	107.5	0.483	0.2	0.342
MBT	6.51	130.8	0.155	0.056	0.106
Kopili	6.21	83.9	0.179	0.065	0.122

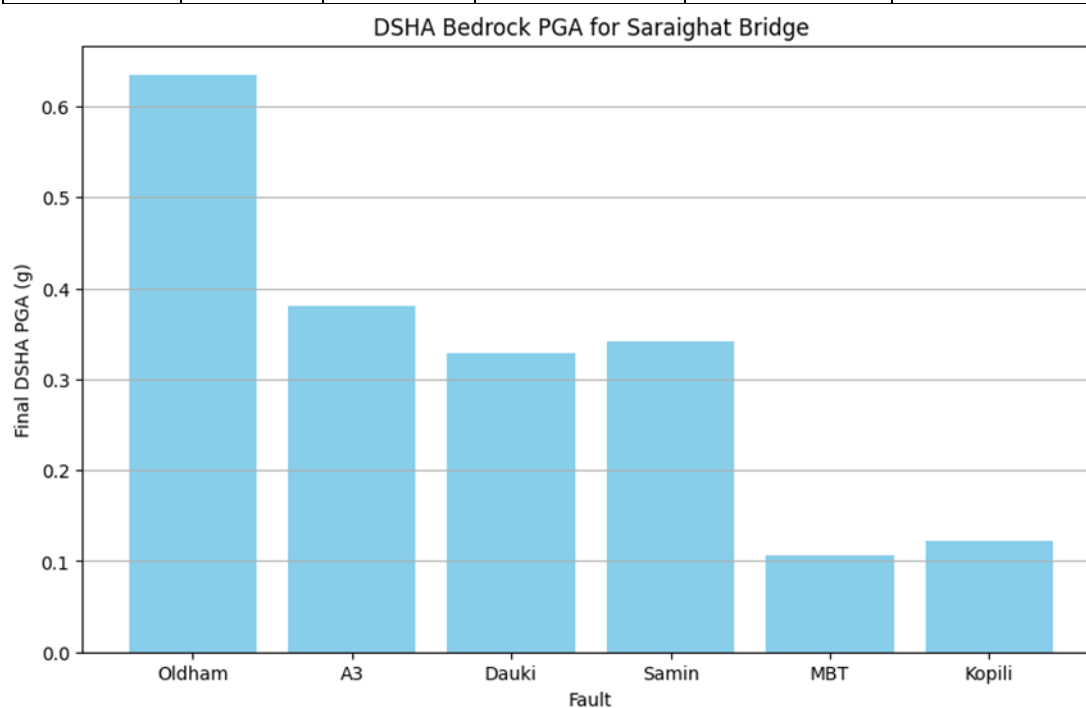


Figure 21 DSHA result for different Faults.

Table 11 Final values of PGA calculated for each fault after amplification (Surface)

Fault	Mmax	Distance (km)	PGA_NDMA (g)	PGA_Bajaj (g)	Final DSHA PGA (g)
Oldham F.	6.46	10.73	0.876	0.394	0.826
A3	7.85	135.3	0.536	0.227	0.495
Dauki F.	7.51	112.9	0.465	0.192	0.426
Samin F.	7.5	107.5	0.483	0.2	0.445
MBT	6.51	130.8	0.155	0.056	0.138
Kopili F.	6.21	83.9	0.179	0.065	0.159
Controlling Fault – Oldham					0.826

The deterministic PGA for each fault was tabulated and compared. The controlling source (the fault contributing the maximum deterministic hazard) was determined, and its PGA was reported as the site-specific deterministic design PGA.

4.11 Conclusion on DSHA results.

The findings indicate that the structural design and retrofitting of the Saraighat Bridge must take into account the Oldham fault scenario as the fundamental design criterion, with a design PGA of roughly 0.826 g. This approach guarantees that the bridge's design considers the most severe possible ground motion anticipated from the active faults in the area.

4.12 Probabilistic Seismic Hazard Assessment (PSHA)

A Probabilistic Seismic Hazard Assessment (PSHA) was conducted to determine the probability of various levels of earthquake-induced ground motion at the location of the Saraighat Bridge over different timeframes. In contrast to the Deterministic Seismic Hazard Assessment (DSHA), which focuses solely on a single worst-case scenario, the PSHA combines the effects of all relevant nearby faults and considers earthquake occurrence to be a random event.

For this analysis, six major faults in proximity to the site were modeled, each with distinct seismicity parameters (a- and b-values) and maximum magnitudes (M_{max}). The minimum distances from each fault to the bridge were calculated through geospatial analysis. Two ground motion prediction equations (NDMA 2011 and Bajaj & Anbazhagan 2019) were employed with equal weighting to estimate bedrock-level Peak Ground Acceleration (PGA) and spectral acceleration.

The PSHA process involves four major steps:

1. Seismic Source Characterization

The study region was divided into multiple seismotectonic source zones based on geological and historical seismicity data. However, for detailed UHS representation and comparison, the Oldham Fault identified as the dominant contributing source was selected for focused analysis.

2. Earthquake Recurrence Modeling

For each fault, the Gutenberg-Richter recurrence relationship was applied to model the frequency of earthquake occurrences:

$$\mathbf{Log_{10}(N) = a - bM}$$

where a and b are seismicity parameters determined from declustered and magnitude-homogenized historical earthquake data. For the Oldham Fault, the parameters were set as $a=2.25$, $b=0.70$, and $M_{\max}=7.8$, with a minimum source-to-site distance of 65 km.

3. Ground Motion Prediction Equations (GMPEs)

To estimate ground shaking intensity, two regionally appropriate GMPEs were used, the NDMA (2011) and Bajaj & Anbazhagan (2019) models. Spectral acceleration values were computed by averaging the results of both GMPEs at varying magnitudes and distances. The logarithmic mean ground motion $\log_{10}(S_a)$ was computed for each magnitude-distance pair, and a standard deviation $\sigma = 0.28$ was used to capture variability.

4. Hazard Integration

The total annual rate of exceedance $\lambda(y^*)$ for a given ground motion level y^* was calculated by integrating over all magnitudes and distances for each fault:

$$\lambda(y^*) = \int_{Mmin}^{Mmax} \int_{Rmin}^{Rmax} \lambda(M) \cdot fM(M) \cdot fR(R) \cdot P[Y > Y^* | M, R] dM dR$$

Equation 5 Hazard Integration (kramer, n.d.)

This process yields the rate at which a particular PGA or spectral acceleration is exceeded at the site.

Uniform Hazard Spectrum (UHS)

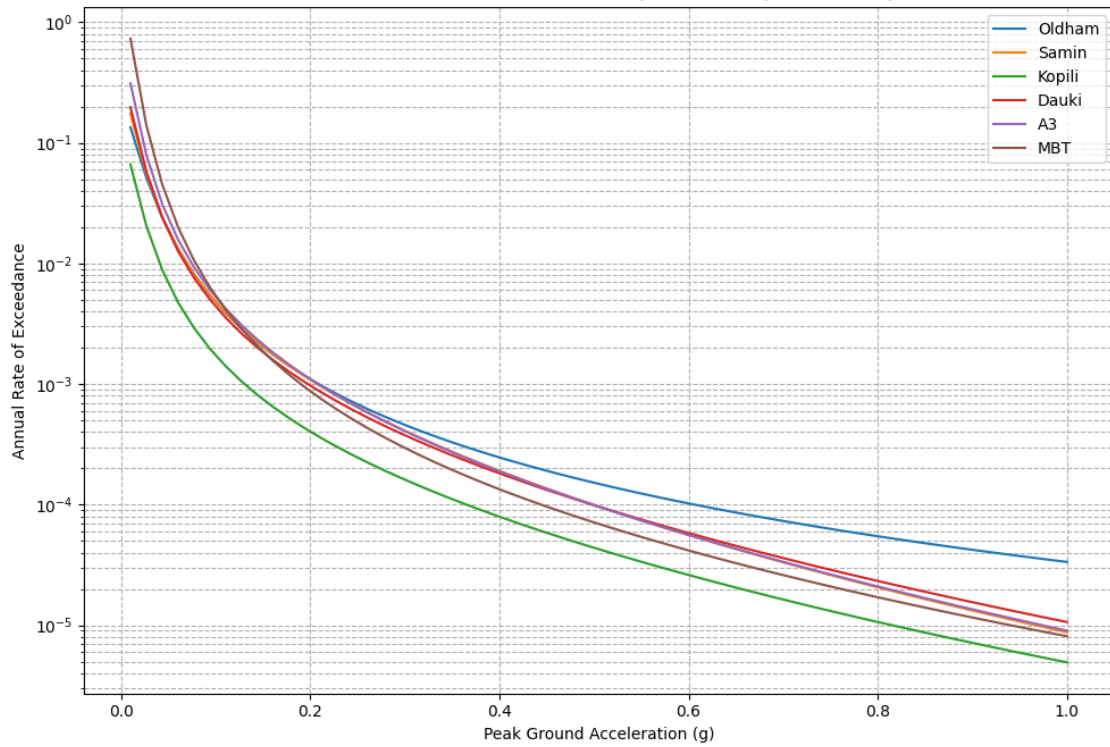
To visualize seismic demand across a range of structural periods, a Uniform Hazard Spectrum (UHS) was developed. This spectrum represents the peak spectral acceleration values at different periods that are expected to be exceeded with a uniform probability over specific return periods. The following return periods were used in the UHS construction:

- 475 years (10% in 50 years)
- 950 years (10% in 100 years)
- 975 years (5% in 50 years)
- 1975 years (5% in 100 years)
- 2475 years (2% in 50 years)

For each case, the PGA was computed from hazard curves for the Oldham Fault using the integrated PSHA framework. The IS 1893:2016 Type II rock-site spectral shape was then scaled using these PGA values to compute spectral acceleration across a period range of 0 to 4 seconds.

Results and Interpretation

The UHS results showed increasing spectral acceleration with longer return periods, as expected. For instance, at a spectral period of 0.2 seconds, the spectral acceleration



value was significantly higher for the 2475-year return period compared to the 475-year spectrum, highlighting the increased ground motion demand during rarer seismic events. The plateau between 0.1 to 0.55 seconds aligns with typical amplification behaviour observed in hard rock sites.

Figure 22 Seismic Hazard Curve for Saraighat Bridge

Fault-wise PGA Bar Chart

The fault-wise bar chart presents the estimated peak ground acceleration (PGA) at bedrock for each of the six primary faults that influence the Saraighat Bridge site. PGA values were gathered for each fault considering different probabilities of exceedance: 2%, 5%, and 10% over both 50-year and 100-year periods.

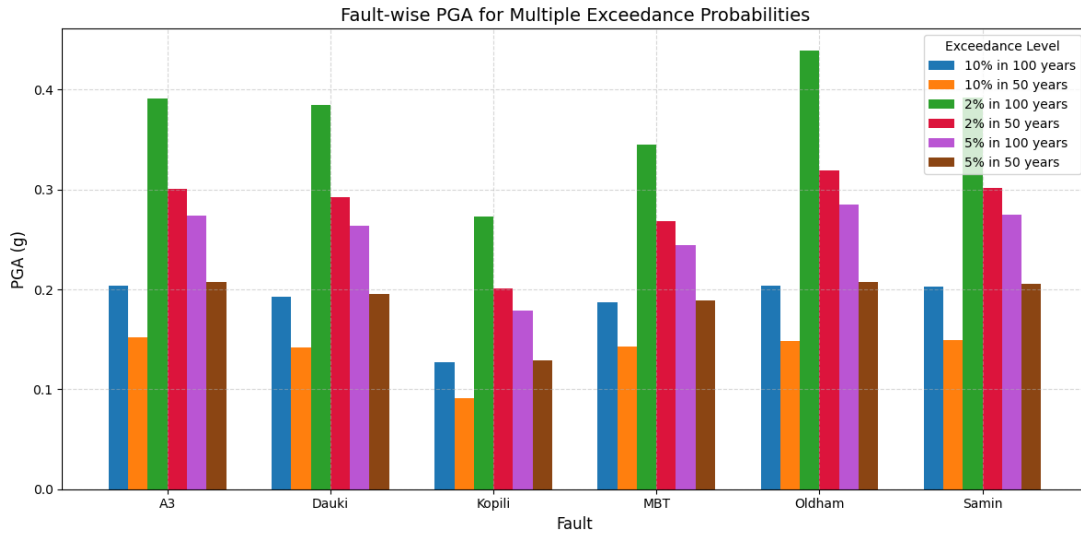


Figure 23 Fault-Wise PGA for Multiple Exceedance Probabilities.

The findings reveal how various faults affect the seismic risk at the site under different levels of exposure. For instance, the Oldham Fault exhibits the highest PGA values in scenarios with low probabilities and high return periods, attributable to its proximity and moderate maximum magnitude. Meanwhile, the A3 and Dauki Faults display notable contributions at extended return periods due to their higher estimated maximum magnitudes, despite their greater distance. The chart illustrates how the primary controlling fault can change based on the design return period, emphasizing the importance of Probabilistic Seismic Hazard Assessment (PSHA) in synthesizing all relevant sources and exceedance probabilities to create a comprehensive hazard assessment for the site.

Design-level ground motions were derived from the overall hazard curve for typical engineering return intervals (such as 10% in 50 years, 5% in 50 years, and 2% in 50

years). The Uniform Hazard Spectrum (UHS) was then developed by applying standardized spectral shape factors to the bedrock PGA, yielding spectral acceleration values for a range of vibration periods.

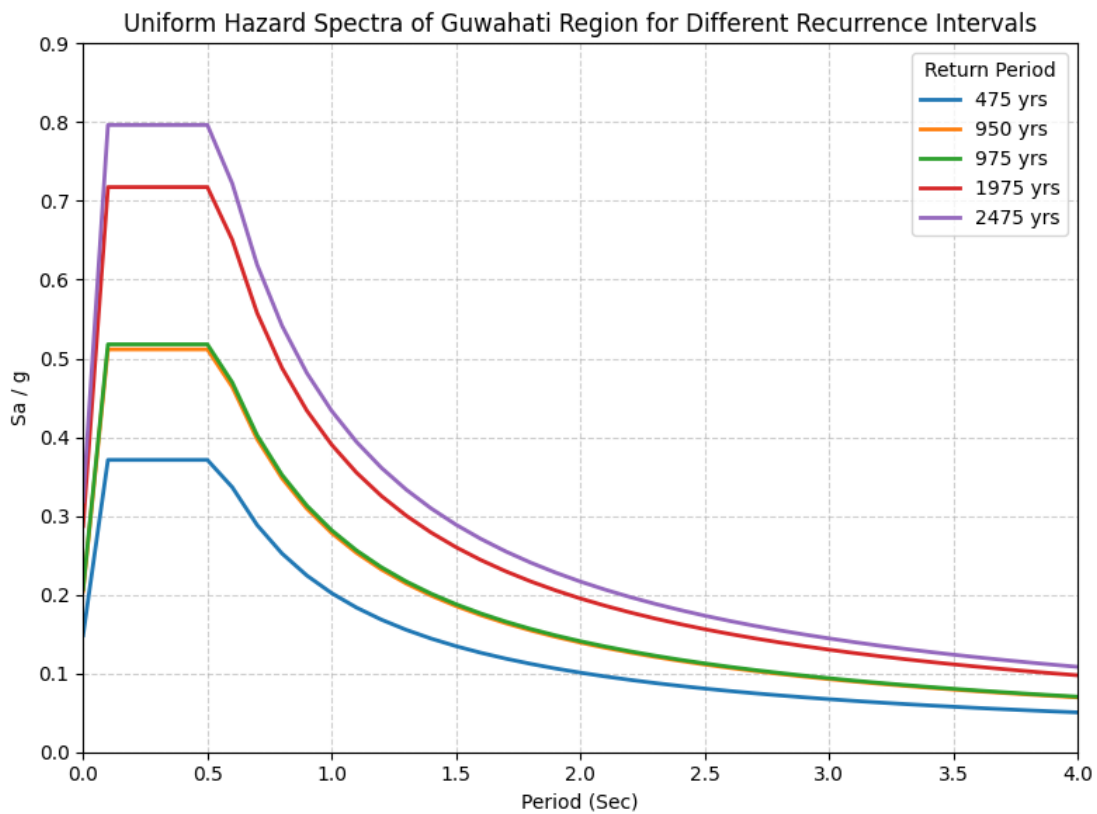


Figure 24 Uniform Hazard Spectrum (UHS) for the Oldham Fault at five return periods (475, 950, 975, 1975, and 2475 years), developed from PSHA and scaled using IS 1893 spectral shape for rock sites.

The UHS provides S_a/g values across a period range of 0–4 seconds for performance-based seismic design. This organized methodology guarantees that both near-field and regional seismic activities are considered when estimating site-specific seismic demands.

Results

Table 12 Fault Wise PGA for multiple exceedance Probabilities.

Fault	10% in 100 years	10% in 50 years	2% in 100 years	2% in 50 years	5% in 100 years	5% in 50 years
A3	0.204	0.152	0.391	0.301	0.274	0.207
Dauki	0.193	0.142	0.385	0.292	0.264	0.195
Kopili	0.127	0.091	0.273	0.201	0.179	0.129
MBT	0.187	0.143	0.345	0.268	0.244	0.189
Oldham	0.204	0.150	0.439	0.319	0.285	0.207
Samin	0.203	0.149	0.392	0.302	0.275	0.206

4.13 Conclusion on PSHA

The PSHA conducted for the study site effectively captured the probabilistic nature of seismic hazard by considering a range of magnitudes, distances, and their associated likelihoods. The Oldham fault should be considered the key fault for seismic design and risk mitigation due to its consistently higher PGA values, especially at the most severe earthquake exceedance probabilities and longer time horizons. This underscores its geological and seismic importance in the Saraighat region. The Oldham Fault, as the

controlling source, was used to develop Uniform Hazard Spectra (UHS) for multiple return periods.

CHAPTER 4

CONCLUSION

This dissertation has presented a comprehensive seismic hazard assessment for the Guwahati region, with a focus on the site of the Saraighat Bridge, by integrating both Deterministic Seismic Hazard Analysis (DSHA) and Probabilistic Seismic Hazard Analysis (PSHA) methodologies. The study utilized a refined earthquake catalogue, fault-specific seismicity parameters, and regionally appropriate Ground Motion Prediction Equations (GMPEs) to provide an updated and site-specific hazard evaluation.

In the deterministic approach, a maximum peak ground acceleration (PGA) value of 0.826g was obtained for the Saraighat Bridge site. This value corresponds to the Oldham Fault, which was identified as the controlling seismic source based on its minimum distance to the site and associated maximum credible magnitude. The DSHA result represents a conservative estimate of the strongest possible shaking the site may experience, and it emphasizes the need for robust earthquake-resistant design for critical infrastructure.

This probabilistic seismic hazard analysis presents fault-specific PGA values at multiple exceedance levels (2%, 5%, and 10% in 50 and 100 years) for the Guwahati region. The Oldham fault emerges as the primary hazard source, with a peak PGA of 0.439g at 2% in 100 years, followed by Samin and A3 faults. At the commonly used 10% in 50 years design level, several faults show PGA values above 0.15g, approaching the IS 1893 (2016) code value of 0.18g for Zone V.

Compared to previous studies, these values fall between conservative estimates (e.g., Nath et al. 0.66g) and lower values from Das et al. (0.24g) and Bandyopadhyay et al. (0.25g), offering a balanced, detailed hazard model for site-specific design. These findings highlight the importance of detailed fault-wise assessments for accurate seismic risk evaluation, supporting safer infrastructure design, land-use planning, and disaster preparedness in this seismically active region.

REFERENCES

- Bahuguna, A., & Sil, A. (2020). Comprehensive Seismicity, Seismic Sources and Seismic Hazard Assessment of Assam, North East India. *Journal of Earthquake Engineering*, 24(2), 254–297. <https://doi.org/10.1080/13632469.2018.1453405>
- Bandyopadhyay, S., Parulekar, Y. M., & Sengupta, A. (2022). Generation of seismic hazard maps for Assam region and incorporation of the site effects. *Acta Geophysica*, 70(5), 1957–1977. <https://doi.org/10.1007/s11600-022-00846-z>
- Beitr, G. , 1945. F. of earthquakes in California. N. 156 (3960), 371. (n.d.). *Gutenberg and Richter law*.
- Das, R., Sharma, M. L., & Wason, H. R. (2016). Probabilistic Seismic Hazard Assessment for Northeast India Region. *Pure and Applied Geophysics*, 173(8), 2653–2670. <https://doi.org/10.1007/s00024-016-1333-9>
- IS 1893:2016 Part I. (2016). *Criteria for Earthquake Resistant Design of Structures Part 1 General Provisions and Buildings (Sixth Revision)*. www.standardsbis.in
- Kijko, A. (2004). Estimation of the maximum earthquake magnitude, m_{max} . *Pure and Applied Geophysics*, 161(8), 1655–1681. <https://doi.org/10.1007/s00024-004-2531-4>
- Kijko, A., & Graham, G. (1998). Parametric-historic Procedure for Probabilistic Seismic Hazard Analysis Part I: Estimation of Maximum Regional Magnitude m_{max} . In *Pure appl. geophys* (Vol. 152).
- kramer. (n.d.). *Geotechnical Earthquake Engineering*.

- Kumar Jaiswal, R., Mukherjee, S., Raju, K. D., & Saxena, R. (2002). Forest fire risk zone mapping from satellite imagery and GIS. In *International Journal of Applied Earth Observation and Geoinformation* (Vol. 4).
- Mishra, S., Kumar, A., & Sil, A. (2024). Comprehensive seismic hazard assessment for Guwahati City, Northeast India: Insights from probabilistic and deterministic seismic hazard analysis. *Natural Hazards Research*, 4(3), 423–433. <https://doi.org/10.1016/j.nhres.2023.10.005>
- Nath, S. K., & Thingbaijam, K. K. S. (2012). Probabilistic seismic hazard assessment of India. *Seismological Research Letters*, 83(1), 135–149. <https://doi.org/10.1785/gssrl.83.1.135>
- Parulekar, Y. M., & Sengupta, A. (2022). Generation of seismic hazard maps for Assam region and incorporation of the site effects. *Acta Geophysica*, 70(5), 1957–1977. <https://doi.org/10.1007/s11600-022-00846-z>
- Sharma, M. L. , M. S. (n.d.). *Sharma, M.L., Malik, Shipra, 2006a. Probabilistic Seismic Hazard Analysis and Estimation.*
- Sil, A., Sitharam, T. G., & Kolathayar, S. (2013). Probabilistic seismic hazard analysis of Tripura and Mizoram states. *Natural Hazards*, 68(2), 1089–1108. <https://doi.org/10.1007/s11069-013-0678-y>
- Sitharam, T. G., & Sil, A. (2014). Comprehensive seismic hazard assessment of Tripura and Mizoram states. *Journal of Earth System Science*, 123(4), 837–857. <https://doi.org/10.1007/s12040-014-0438-8>

APPENDIX A

STEPS TO PERFORM DETERMINISTIC SEISMIC HAZARD ASSESSMENT

(DSHA) USING PYTHON

```
from google.colab import files
uploaded = files.upload()
Homogenized_Earthquake_Catalogue__Mw_.csv
• Homogenized_Earthquake_Catalogue__Mw_.csv(text/csv) - 48447 bytes, last
modified: 27/06/2025 - 100% done
Saving Homogenized_Earthquake_Catalogue__Mw_.csv to
Homogenized_Earthquake_Catalogue__Mw_.csv
```

```
import pandas as pd
from shapely.geometry import LineString, Point
from google.colab import files

# STEP 1: Loading our catalogue
catalog =
pd.read_csv('Homogenized_Earthquake_Catalogue__Mw_.csv')
catalog['ID'] = catalog.index + 1 # Add ID if needed

# STEP 2: Defining faults
faults = {
    'Oldham': [(91.73, 26.11), (90.72, 25.77)],
    'Kopili': [(92.5, 26.0), (93.5, 27.5)],
    'Dauki': [(92.97, 25.12), (89.94, 25.26)],
    'Samir': [(90.53, 25.76), (90.67, 25.90)],
    'A3': [(93.04, 26.31), (93.65, 26.48)],
    'MBT': [(93.00, 25.50), (93.00, 27.50)]
}

# STEP 3: Assigning events
assigned = []

for _, row in catalog.iterrows():
    eq_point = Point(row['Longitude'], row['Latitude'])
    for fault_name, coords in faults.items():
        fault_line = LineString(coords)
        distance_km = eq_point.distance(fault_line) * 111 #
(Approx degrees to km)
        if distance_km <= 50:
            assigned.append({
                'EventID': row['ID'],
                'Date': row['Date'],
                'Longitude': row['Longitude'],
                'Latitude': row['Latitude'],
                'Mw': row['Mw'],
```

```

        'Fault': fault_name,
        'Distance_km': round(distance_km, 2)
    })

# STEP 4: Saving full assignments
assigned_df = pd.DataFrame(assigned)
assigned_df.to_csv('Fault_Assignment.csv', index=False)

# Also saving summary
summary =
assigned_df.groupby('Fault').size().reset_index(name='Events
Assigned')
summary.to_csv('Fault_Event_Counts.csv', index=False)

print(summary)

# STEP 5: Make it downloadable
files.download('Fault_Assignment.csv')
files.download('Fault_Event_Counts.csv')

```

	Fault	Events Assigned
0	A3	57
1	Dauki	75
2	Kopili	84
3	MBT	100
4	Oldham	61
5	Samin	40

```

# FAULT-WISE G-R FIT

import pandas as pd
import numpy as np
import matplotlib.pyplot as plt
from scipy.stats import linregress
from google.colab import files

# STEP 1: Uploading our Fault_Assignment CSV

uploaded = files.upload()

# File name must match exactly
df = pd.read_csv('Fault_Assignment.csv')
df['Mw'] = pd.to_numeric(df['Mw'], errors='coerce')

# STEP 2: Adding ID or Year if missing

if 'ID' not in df.columns:
    df['ID'] = df.index + 1

```

```

if 'Date' in df.columns:
    df['Year'] = pd.to_datetime(df['Date'],
errors='coerce').dt.year
else:
    raise ValueError("No 'Date' column found!")

# STEP 3: Define completeness periods

completeness = {
    '4.0-4.9': 1976,
    '5.0-5.9': 1931,
    '6.0-6.9': 1939,
    '7.0+': 1918
}

def get_completeness_year(mw):
    if mw >= 7.0:
        return completeness['7.0+']
    elif mw >= 6.0:
        return completeness['6.0-6.9']
    elif mw >= 5.0:
        return completeness['5.0-5.9']
    else:
        return completeness['4.0-4.9']

# STEP 4: Loop, filter, fit G-R, plot

results = []

for fault in df['Fault'].unique():
    fault_df = df[df['Fault'] == fault].copy()
    fault_df['Completeness_Year'] =
fault_df['Mw'].apply(get_completeness_year)
    fault_df = fault_df[(fault_df['Year'] >=
fault_df['Completeness_Year']) & (fault_df['Mw'] >= 4.0)]

    if len(fault_df) < 5:
        print(f"Skipping {fault}: not enough complete events.")
        continue

    Mw_bins = np.linspace(4.0, fault_df['Mw'].max(),
num=int((fault_df['Mw'].max() - 4.0) / 0.1) + 1)
    counts = [sum(fault_df['Mw'] >= Mw) for Mw in Mw_bins]
    counts = np.array(counts)
    valid = counts > 0

    logN = np.log10(counts[valid])

```

```

Mw_valid = Mw_bins[valid]

slope, intercept, _, _, _ = linregress(Mw_valid, logN)
b_value = round(-slope, 3)
a_value = round(intercept, 3)

results.append({
    'Fault': fault,
    'a': a_value,
    'b': b_value,
    'N_events': len(fault_df)
})

# Plot + save
plt.figure()
plt.scatter(Mw_valid, logN, label='Data', color='blue')
plt.plot(Mw_valid, intercept + slope * Mw_valid, 'r--',
label=f'Fit: a={a_value}, b={b_value}')
plt.xlabel('Magnitude Mw')
plt.ylabel('log10(N ≥ Mw)')
plt.title(f'Gutenberg-Richter: {fault}')
plt.legend()
plt.grid(True)
plt.savefig(f'GR_{fault}.png', dpi=300)
plt.close()

# STEP 5: Saving table

gr_df = pd.DataFrame(results)
gr_df.to_csv('GR_Faultwise.csv', index=False)

print("Final G-R results:")
print(gr_df)
print("All PNG plots saved. Table saved as GR_Faultwise.csv ")
from google.colab import files

# Downloads the CSV table
files.download('GR_Faultwise.csv')

import shutil

# Makes a zip of all GR_*.png files
!zip GR_Plots.zip GR_*.png

# Downloads the zip
files.download('GR_Plots.zip')

```

• **Fault_Assignment (1).csv**(text/csv) - 29174 bytes, last modified: 08/09/2025 - 100% done

Saving Fault_Assignment (1).csv to Fault_Assignment (1).csv

Final G-R results:

	Fault	a	b	N_events
0	Dauki	5.614	0.856	71
1	Samin	5.600	0.929	39
2	Oldham	5.875	0.947	60
3	A3	4.856	0.735	55
4	Kopili	6.099	0.960	80
5	MBT	6.555	1.039	97

All PNG plots saved. Table saved as GR_Faultwise.csv

```
adding: GR_A3.png (deflated 15%)
adding: GR_Dauki.png (deflated 15%)
adding: GR_Kopili.png (deflated 16%)
adding: GR_MBT.png (deflated 15%)
adding: GR_Oldham.png (deflated 15%)
adding: GR_Samin.png (deflated 15%)
```

```
# Saraighat Mmax & Distance Calculator
```

```
import pandas as pd
import numpy as np
from shapely.geometry import LineString, Point
from geopy.distance import geodesic

# 1 Load our Fault_Assignment.csv

from google.colab import files
uploaded = files.upload()

df = pd.read_csv('Fault_Assignment.csv')

# Ensure numeric Mw
df['Mw'] = pd.to_numeric(df['Mw'], errors='coerce')

# 2 Add Gutenberg-Richter b-values per fault
# Replace with our final fitted b-values!

b_values = {
    'Oldham': 0.95,
    'A3': 0.75,
    'Dauki': 0.85,
    'Samin': 0.93,
    'MBT': 1.03,
    'Kopili': 0.96
}
```

```

# 3 Calculate Mobs, Mmax_Kijko, Mmax_Jaiswal for each fault

mmax_results = []

for fault in df['Fault'].unique():
    fault_df = df[df['Fault'] == fault]
    Mobs = fault_df['Mw'].max()
    b = b_values[fault]

    Mmax_Jaiswal = Mobs + 0.5
    Mmax_Kijko = Mobs + (0.5 / b)
    Mmax_final = round(max(Mmax_Jaiswal, Mmax_Kijko), 2)

    mmax_results.append({
        'Fault': fault,
        'Max Observed Mw': round(Mobs, 2),
        'b-value': b,
        'Mmax Jaiswal': round(Mmax_Jaiswal, 2),
        'Mmax Kijko': round(Mmax_Kijko, 2),
        'Final Mmax': Mmax_final
    })

mmax_df = pd.DataFrame(mmax_results)
print("\n Mmax Table:")
print(mmax_df)

# 4 Calculate minimum distance from each fault to Saraighat
Bridge

# Saraighat Bridge location
bridge_point = Point(91.691, 26.200)

# Fault coordinates (lon, lat)
faults = {
    'Oldham': [(91.73, 26.11), (90.72, 25.77)],
    'A3': [(93.04, 26.31), (93.65, 26.48)],
    'Dauki': [(92.97, 25.12), (89.94, 25.26)],
    'Samin': [(90.53, 25.76), (90.67, 25.90)],
    'MBT': [(93.00, 25.50), (93.00, 27.50)],
    'Kopili': [(92.5, 26.0), (93.5, 27.5)]
}

distance_results = []

for fault, coords in faults.items():
    line = LineString(coords)
    projected = line.interpolate(line.project(bridge_point))

```

```

min_dist_km = geodesic((bridge_point.y, bridge_point.x),
(projected.y, projected.x)).km

distance_results.append({
    'Fault': fault,
    'Min Distance (km)': round(min_dist_km, 2)
})

distance_df = pd.DataFrame(distance_results)
print("\n Minimum Distances:")
print(distance_df)

# 5 Merge Mmax and Distance - final DSHA input

final_df = pd.merge(mmax_df, distance_df, on='Fault')
print("\n Final DSHA Input Table:")
print(final_df)

# 6 Save & Download CSV in Colab

final_df.to_csv('Mmax_Distance_Table.csv', index=False)
files.download('Mmax_Distance_Table.csv')

```

Saving Fault_Assignment.csv to Fault_Assignment.csv

Mmax Table:

	Fault	Max Observed Mw	b-value	Mmax Jaiswal	Mmax Kijko	Final Mmax
0	Dauki	6.92	0.85	7.42	7.51	7.51
1	Samini	6.96	0.93	7.46	7.50	7.50
2	Oldham	5.93	0.95	6.43	6.46	6.46
3	A3	7.18	0.75	7.68	7.85	7.85
4	Kopili	5.69	0.96	6.19	6.21	6.21
5	MBT	6.01	1.03	6.51	6.50	6.51

Minimum Distances:

	Fault	Min Distance (km)
0	Oldham	10.73
1	A3	135.32
2	Dauki	112.96
3	Samini	107.45
4	MBT	130.83
5	Kopili	83.90

Final DSHA Input Table:

	Fault	Max Observed Mw	b-value	Mmax Jaiswal	Mmax Kijko	Final Mmax
0	Dauki	6.92	0.85	7.42	7.51	7.51
1	Samini	6.96	0.93	7.46	7.50	7.50
2	Oldham	5.93	0.95	6.43	6.46	6.46
3	A3	7.18	0.75	7.68	7.85	7.85
4	Kopili	5.69	0.96	6.19	6.21	6.21
5	MBT	6.01	1.03	6.51	6.50	6.51

Min Distance (km)

0	112.96
1	107.45
2	10.73

```

3           135.32
4           83.90
5           130.83

```

```

import numpy as np
import pandas as pd
import matplotlib.pyplot as plt

# 1 Fault-wise Mmax and distances (km)

data = [
    {'Fault': 'Oldham', 'Mmax': 7.8, 'Distance_km': 64.9},
    {'Fault': 'A3',      'Mmax': 6.5, 'Distance_km': 175.3},
    {'Fault': 'Dauki',  'Mmax': 6.6, 'Distance_km': 134.9},
    {'Fault': 'Samin',  'Mmax': 6.3, 'Distance_km': 125.5},
    {'Fault': 'MBT',    'Mmax': 7.0, 'Distance_km': 214.8},
    {'Fault': 'Kopili', 'Mmax': 6.6, 'Distance_km': 129.9},
]

df = pd.DataFrame(data)

# 2 NDMA (2011) coefficients
# ln(Y) = a + bM + c*ln(R + d)

ndma = {'a': -1.962, 'b': 0.953, 'c': -1.21, 'd': 25}

# 3 Bajaj & Anbazhagan (2019) coefficients
# ln(Y) = a + bM + c*ln(R + d)

bajaj = {'a': -3.512, 'b': 1.065, 'c': -1.255, 'd': 20}

# 4 Calculate PGA for each GMPE and final average

results = []

for _, row in df.iterrows():
    M = row['Mmax']
    R = row['Distance_km']

    lnPGA_ndma = ndma['a'] + ndma['b'] * M + ndma['c'] * np.log(R
+ ndma['d'])
    PGA_ndma = np.exp(lnPGA_ndma)

    lnPGA_bajaj = bajaj['a'] + bajaj['b'] * M + bajaj['c'] *
np.log(R + bajaj['d'])
    PGA_bajaj = np.exp(lnPGA_bajaj)

```

```

PGA_final = 0.5 * (PGA_ndma + PGA_bajaj)

results.append({
    'Fault': row['Fault'],
    'Mmax': M,
    'Distance (km)': R,
    'PGA_NDMA (g)': round(PGA_ndma, 3),
    'PGA_Bajaj (g)': round(PGA_bajaj, 3),
    'Final DSHA PGA (g)': round(PGA_final, 3)
})

# 5 Make final DataFrame

ds_df = pd.DataFrame(results)
print(ds_df)

# Save as CSV
ds_df.to_csv('DSHA_Results.csv', index=False)

# 6 Show controlling source

max_pga = ds_df.loc[ds_df['Final DSHA PGA (g)'].idxmax()]
print(f"\n Controlling Fault: {max_pga['Fault']} with PGA
{max_pga['Final DSHA PGA (g)']} g")

# 7 Plot DSHA PGA as bar chart

plt.figure(figsize=(10, 6))
plt.bar(ds_df['Fault'], ds_df['Final DSHA PGA (g)'],
color='skyblue')
plt.xlabel('Fault')
plt.ylabel('Final DSHA PGA (g)')
plt.title('DSHA Bedrock PGA for Saraighat Bridge')
plt.grid(axis='y')
plt.show()

# 8 Download CSV (Colab)

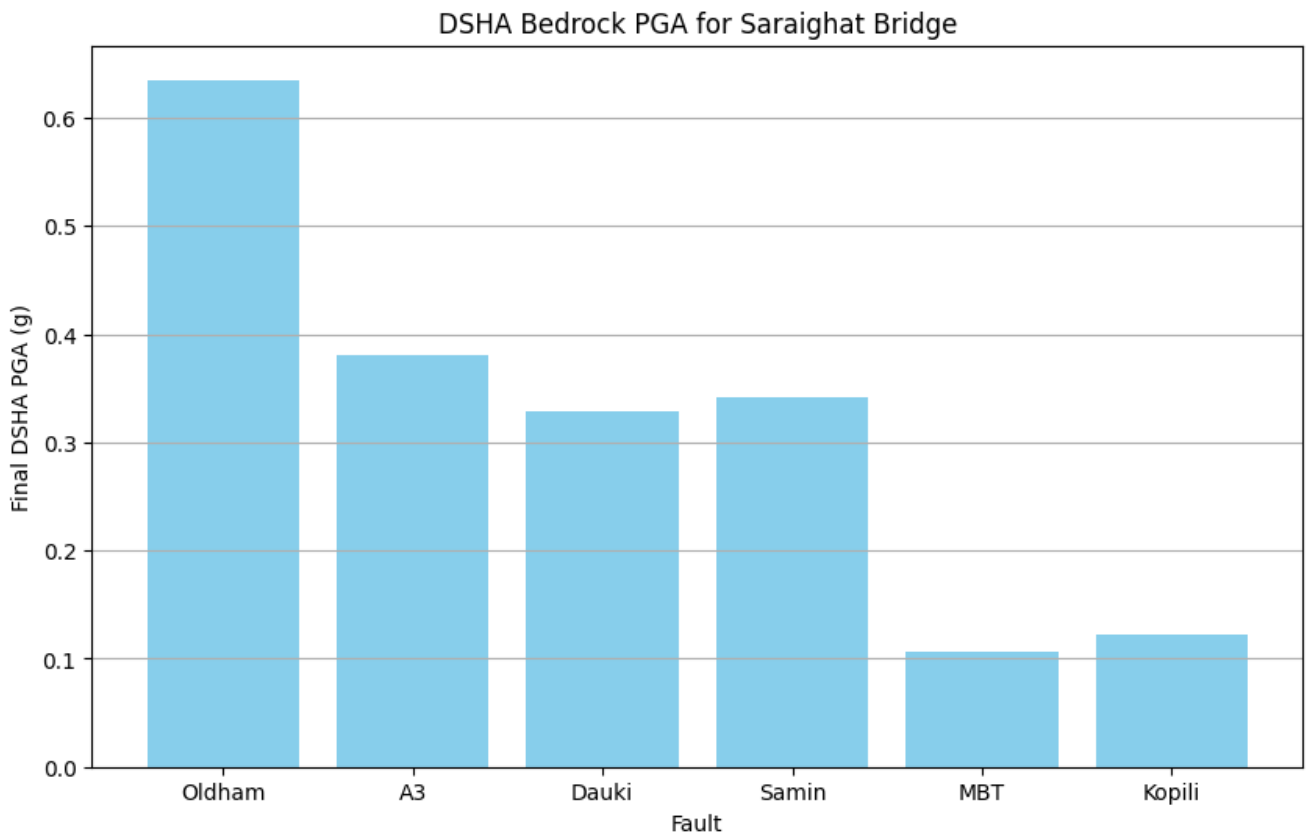
from google.colab import files
files.download('DSHA_Results.csv')

```

Fault	Mmax	Distance (km)	PGA_NDMA (g)	PGA_Bajaj (g)	\
0	Oldham	6.46	10.73	0.876	0.394
1	A3	7.85	135.30	0.536	0.227
2	Dauki	7.51	112.90	0.465	0.192

3	Samín	7.50	107.50	0.483	0.200
4	MBT	6.51	130.80	0.155	0.056
5	Kopili	6.21	83.90	0.179	0.065

Final DSHA PGA (g)	
0	0.635
1	0.381
2	0.328
3	0.342
4	0.106
5	0.122



Controlling Fault: Oldham with PGA 0.635 g

```
import pandas as pd
from google.colab import files

# 1 Upload our final DSHA results table

uploaded = files.upload()
df = pd.read_csv('DSHA_Results.csv')

print(" Original DSHA table:")
print(df)

# 2 Define soil amplification factors
```

```

# For Site Class D (NE India soft to medium alluvium)
# Typical factor: ~1.3 for PGA (rock - surface)

soil_factor = 1.3

# Add column for surface PGA
df['Surface DSHA PGA (g)'] = (df['Final DSHA PGA (g)'] *
soil_factor).round(3)

print("\n Soil-adjusted DSHA table:")
print(df)

# 3 Find controlling fault at surface

max_surface = df.loc[df['Surface DSHA PGA (g)'].idxmax()]
print(f"\n Controlling Fault (Surface): {max_surface['Fault']}
with PGA {max_surface['Surface DSHA PGA (g)']} g")

# 4 Save new table and download

df.to_csv('DSHA_Surface_Results.csv', index=False)
files.download('DSHA_Surface_Results.csv')

```

• **DSHA_Results.csv**(text/csv) - 274 bytes, last modified: 08/09/2025 - 100% done

Saving DSHA_Results.csv to DSHA_Results (1).csv

Original DSHA table:

	Fault	Mmax	Distance (km)	PGA_NDMA (g)	PGA_Bajaj (g)	\
0	Oldham	6.46	10.73	0.876	0.394	
1	A3	7.85	135.30	0.536	0.227	
2	Dauki	7.51	112.90	0.465	0.192	
3	Samin	7.50	107.50	0.483	0.200	
4	MBT	6.51	130.80	0.155	0.056	
5	Kopili	6.21	83.90	0.179	0.065	

Final DSHA PGA (g)

0	0.635
1	0.381
2	0.328
3	0.342
4	0.106
5	0.122

\n Soil-adjusted DSHA table:

	Fault	Mmax	Distance (km)	PGA_NDMA (g)	PGA_Bajaj (g)	\
0	Oldham	6.46	10.73	0.876	0.394	
1	A3	7.85	135.30	0.536	0.227	
2	Dauki	7.51	112.90	0.465	0.192	
3	Samin	7.50	107.50	0.483	0.200	
4	MBT	6.51	130.80	0.155	0.056	
5	Kopili	6.21	83.90	0.179	0.065	

Final DSHA PGA (g) Surface DSHA PGA (g)

0	0.635	0.826
1	0.381	0.495
2	0.328	0.426
3	0.342	0.445
4	0.106	0.138

5

0.122

0.159

Controlling Fault (Surface): Oldham with PGA 0.826 g

APPENDIX B

STEPS TO PERFORM PROBABILISTIC SEISMIC HAZARD ASSESSMENT (PSHA) USING PYTHON

```
import numpy as np
import matplotlib.pyplot as plt
from scipy.stats import norm
from scipy.interpolate import interp1d
import pandas as pd

# Step 1: Define Fault Parameters

faults = {
    'Oldham': {'a': 2.25, 'b': 0.70, 'Mmax': 7.8, 'Rmin': 65},
    'Samain': {'a': 2.17, 'b': 0.64, 'Mmax': 6.3, 'Rmin': 125},
    'Kopili': {'a': 1.8, 'b': 0.65, 'Mmax': 6.6, 'Rmin': 130},
    'Dauki': {'a': 2.4, 'b': 0.68, 'Mmax': 6.6, 'Rmin': 135},
    'A3': {'a': 2.73, 'b': 0.70, 'Mmax': 6.5, 'Rmin': 175},
    'MBT': {'a': 3.8, 'b': 0.85, 'Mmax': 7.0, 'Rmin': 215}
}

# Step 2: Define GMPEs

def gmpe_ndma(M, R):
    log_sa = -2.0 + 0.45 * M - 0.0012 * R - 0.3 * np.log10(R)
    sigma = 0.28
    return log_sa, sigma

def gmpe_bajaj(M, R):
    log_sa = -3.2 + 0.85 * M - 1.35 * np.log10(R + 20)
    sigma = 0.28
    return log_sa, sigma

# Step 3: PDFs

def fM(m, b, Mmin, Mmax):
    beta = 2.303 * b
    norm_factor = 1 - np.exp(-beta * (Mmax - Mmin))
    return (beta * np.exp(-beta * (m - Mmin))) / norm_factor

def fR(r, Rmin, Rmax):
    return 1 / (Rmax - Rmin) if Rmin < r < Rmax else 0

# Step 4: PSHA Integration
```

```

def compute_lambda_y_star_fault(y_star, fault, Mmin=4.0,
Mstep=0.2, Rstep=5.0):
    params = faults[fault]
    a, b, Mmax, Rmin = params['a'], params['b'], params['Mmax'],
params['Rmin']
    alpha = np.log(10) * a

    lambda_fault = 0
    Mvals = np.arange(Mmin, 9.0, Mstep)
    Rvals = np.arange(5, 250, Rstep)

    for M in Mvals:
        if M > Mmax:
            continue
        f_m = fM(M, b, Mmin, Mmax)
        for R in Rvals:
            if R < Rmin:
                continue
            f_r = fR(R, Rmin, max(Rvals))

            mu1, sigma1 = gmpe_ndma(M, R)
            mu2, sigma2 = gmpe_bajaj(M, R)
            mu = (mu1 + mu2) / 2
            sigma = (sigma1 + sigma2) / 2

            log_y = np.log10(y_star)
            p_exceed = 1 - norm.cdf(log_y, mu, sigma)

            rate = np.exp(alpha - np.log(10) * b * M)
            dL = Mstep * Rstep
            lambda_fault += rate * p_exceed * f_m * f_r * dL
    return lambda_fault

# Step 5: Compute Hazard Curves

pga_vals = np.linspace(0.01, 1.0, 60)
fault_curves = {}

for fault in faults:
    lambda_vals = [compute_lambda_y_star_fault(y, fault) for y in
pga_vals]
    fault_curves[fault] = lambda_vals

# Step 6: Plot Hazard Curves

plt.figure(figsize=(10,7))

```

```

for fault, lambdas in fault_curves.items():
    plt.semilogy(pga_vals, lambdas, label=fault)

plt.xlabel("Peak Ground Acceleration (g)")
plt.ylabel("Annual Rate of Exceedance")
plt.title("Seismic Hazard Curve for All Faults")
plt.grid(True, which='both', linestyle='--')
plt.legend()
plt.tight_layout()
plt.show()

# Step 7: Compute PGA at Exceedance Levels

def annual_rate(prob, years): return -np.log(1 - prob) / years

targets = {
    "2% in 50 years": annual_rate(0.02, 50),
    "5% in 50 years": annual_rate(0.05, 50),
    "10% in 50 years": annual_rate(0.10, 50),
    "2% in 100 years": annual_rate(0.02, 100),
    "5% in 100 years": annual_rate(0.05, 100),
    "10% in 100 years": annual_rate(0.10, 100)
}

pga_at_target = {}
for fault, lambdas in fault_curves.items():
    interp_func = interp1d(lambdas[::-1], pga_vals[::-1],
fill_value="extrapolate")
    pga_at_target[fault] = {label: float(interp_func(rate)) for
label, rate in targets.items()}

# Step 8: Create Summary Table

rows = []
for level in targets:
    level_data = {fault: round(pga_at_target[fault][level], 3)
for fault in faults}
    controlling_fault = max(level_data, key=level_data.get)
    for fault, pga in level_data.items():
        rows.append({
            "Exceedance Level": level,
            "Fault": fault,
            "PGA (g)": pga,
            "Controlling Source": "Yes" if fault ==
controlling_fault else "No"
        })

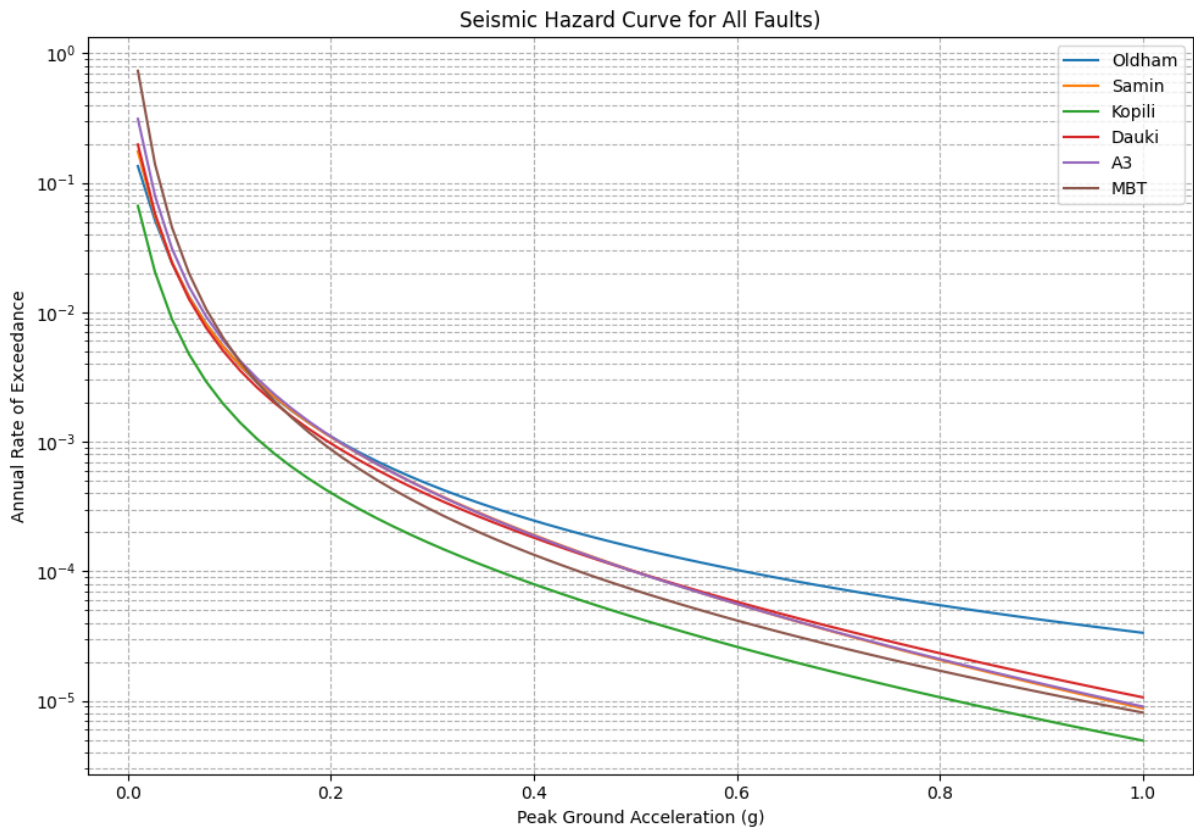
```

```

df_final = pd.DataFrame(rows)
df_pivot = df_final.pivot(index="Fault", columns="Exceedance
Level", values="PGA (g)")
df_pivot["Controlling Fault Count"] =
df_final[df_final["Controlling Source"] ==
"Yes"]["Fault"].value_counts()
df_pivot.fillna(0, inplace=True)

# Display the final summary table
print(" Final PGA Values")
display(df_pivot)

```



Final PGA Values

Exceedance Level	10% in 100 years	10% in 50 years	2% in 100 years	2% in 50 years	5% in 100 years	5% in 50 years	Controlling Fault Count
Fault							
A3	0.204	0.152	0.391	0.301	0.274	0.207	1.0
Dauki	0.193	0.142	0.385	0.292	0.264	0.195	0.0
Kopili	0.127	0.091	0.273	0.201	0.179	0.129	0.0
MBT	0.187	0.143	0.345	0.268	0.244	0.189	0.0
Oldham	0.204	0.150	0.439	0.319	0.285	0.207	5.0

Exceedance Level	10% in 100 years	10% in 50 years	2% in 100 years	2% in 50 years	5% in 100 years	5% in 50 years	Controlling Fault Count
Fault							
Samin	0.203	0.149	0.392	0.302	0.275	0.206	0.0

```

import matplotlib.pyplot as plt
import numpy as np

# Remove 'Controlling Fault Count' from plotting
labels = [col for col in df_pivot.columns if "Controlling" not in col]
faults = df_pivot.index.tolist()
data = [df_pivot[col].values for col in labels]

# Bar setup
x = np.arange(len(faults))
width = 0.12
colors = ['tab:blue', 'tab:orange', 'tab:green', 'crimson',
          'mediumorchid', 'saddlebrown']

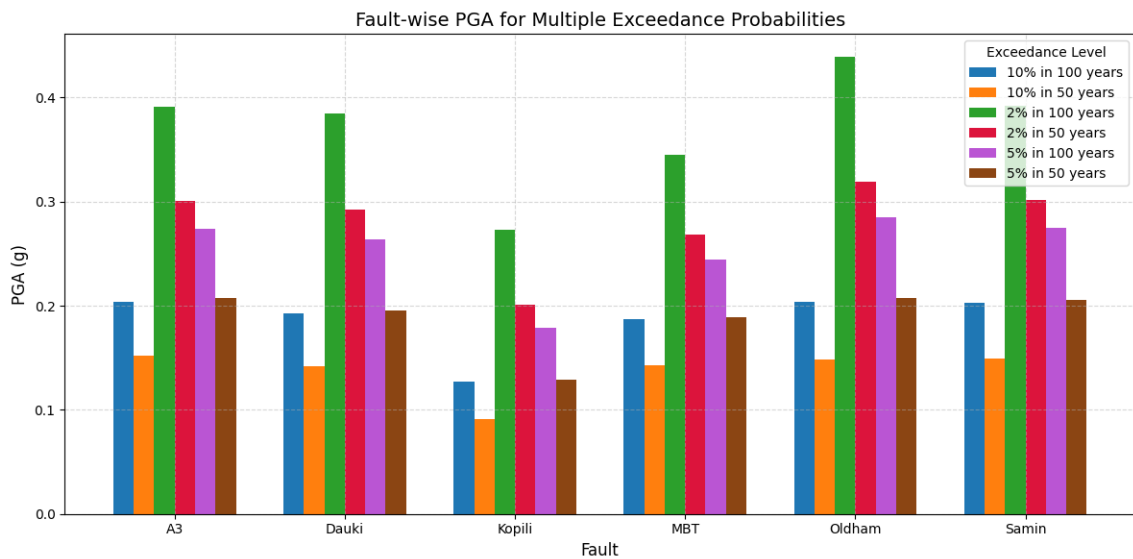
fig, ax = plt.subplots(figsize=(12, 6))

for i, (label, values) in enumerate(zip(labels, data)):
    ax.bar(x + i*width, values, width, label=label,
          color=colors[i % len(colors)])

# Labeling
ax.set_xlabel('Fault', fontsize=12)
ax.set_ylabel('PGA (g)', fontsize=12)
ax.set_title('Fault-wise PGA for Multiple Exceedance
Probabilities', fontsize=14)
ax.set_xticks(x + width * (len(labels) - 1) / 2)
ax.set_xticklabels(faults)
ax.legend(title='Exceedance Level', fontsize=10)
ax.grid(True, linestyle='--', alpha=0.5)

plt.tight_layout()
plt.show()

```



```

import numpy as np
import matplotlib.pyplot as plt
from scipy.stats import norm
from scipy.interpolate import interp1d

# Oldham Fault Parameters
oldham_params = {'a': 2.25, 'b': 0.70, 'Mmax': 7.8, 'Rmin': 65}

# GMPEs
def gmpe_ndma(M, R):
    log_sa = -2.0 + 0.45 * M - 0.0012 * R - 0.3 * np.log10(R)
    return log_sa, 0.28

def gmpe_bajaj(M, R):
    log_sa = -3.2 + 0.85 * M - 1.35 * np.log10(R + 20)
    return log_sa, 0.28

# PDF Functions
def fM(m, b, Mmin, Mmax):
    beta = 2.303 * b
    norm_factor = 1 - np.exp(-beta * (Mmax - Mmin))
    return (beta * np.exp(-beta * (m - Mmin))) / norm_factor

def fR(r, Rmin, Rmax):
    return 1 / (Rmax - Rmin) if Rmin < r < Rmax else 0

# PSHA Integration for Oldham Fault
def compute_lambda_y_star_oldham(y_star, Mmin=4.0, Mstep=0.2,
Rstep=5.0):
    a, b, Mmax, Rmin = oldham_params['a'], oldham_params['b'],
oldham_params['Mmax'], oldham_params['Rmin']
    alpha = np.log(10) * a

```

```

lambda_total = 0

Mvals = np.arange(Mmin, 9.0, Mstep)
Rvals = np.arange(5, 250, Rstep)

for M in Mvals:
    if M > Mmax:
        continue
    f_m = fM(M, b, Mmin, Mmax)
    for R in Rvals:
        if R < Rmin:
            continue
        f_r = fR(R, Rmin, max(Rvals))
        mu1, sigma1 = gmpe_ndma(M, R)
        mu2, sigma2 = gmpe_bajaj(M, R)
        mu = (mu1 + mu2) / 2
        sigma = (sigma1 + sigma2) / 2

        log_y = np.log10(y_star)
        p_exceed = 1 - norm.cdf(log_y, mu, sigma)

        rate = np.exp(alpha - np.log(10) * b * M)
        dL = Mstep * Rstep
        lambda_total += rate * p_exceed * f_m * f_r * dL
return lambda_total

# Return Periods and Target Exceedance Rates
return_periods = {
    "475 yrs": 475,
    "950 yrs": 950,
    "975 yrs": 975,
    "1975 yrs": 1975,
    "2475 yrs": 2475
}
target_lambdas = {label: 1.0 / rp for label, rp in
return_periods.items()}

pga_vals = np.linspace(0.01, 1.5, 80)
lambda_vals = [compute_lambda_y_star_oldham(y) for y in pga_vals]
interp_func = interp1d(lambda_vals[::-1], pga_vals[::-1],
fill_value="extrapolate")
pga_dict = {label: float(interp_func(rate)) for label, rate in
target_lambdas.items()}

# Define Spectral Periods from 0 to 4 sec
periods = np.round(np.linspace(0.0, 4.0, 41), 2)

# Compute UHS Using IS 1893 Style Shape
Sa_extended = {}

```

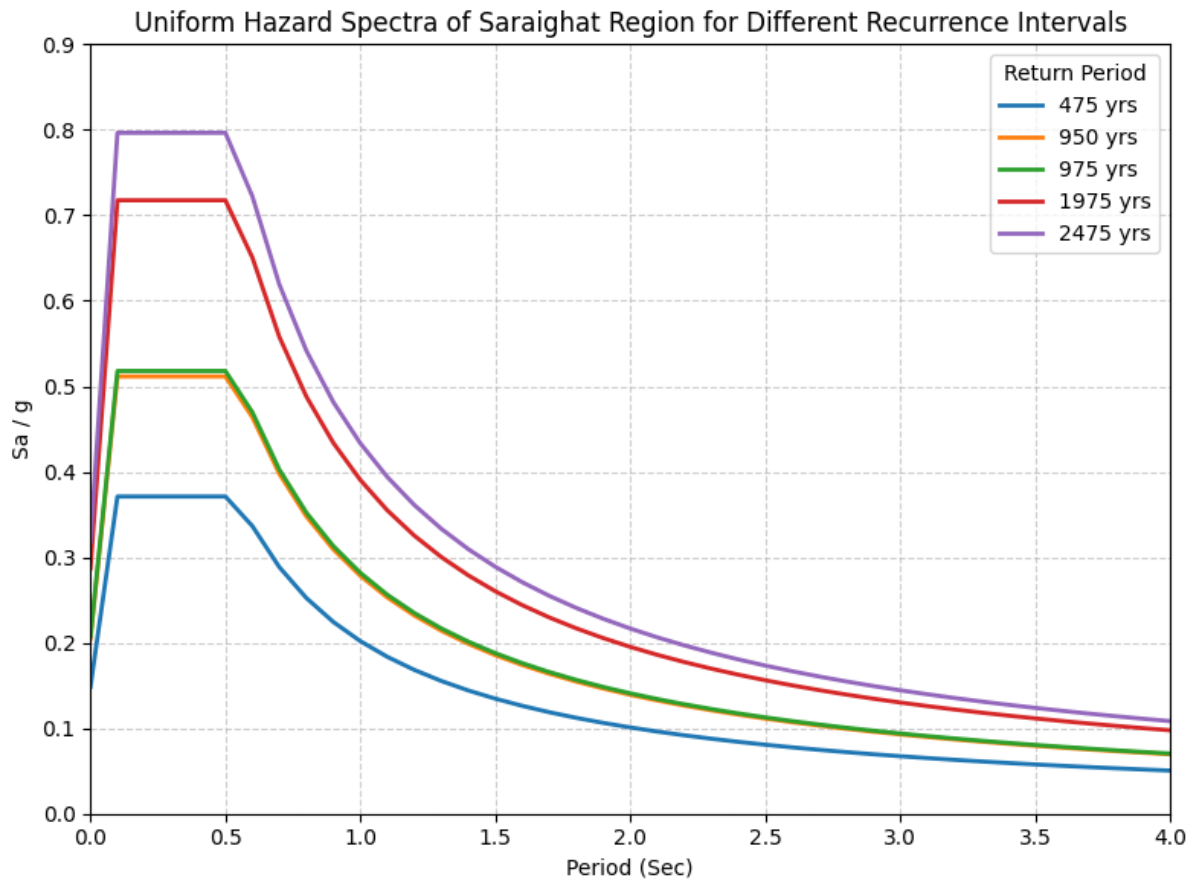
```

for label, pga in pga_dict.items():
    sa_vals = []
    for T in periods:
        if T <= 0.1:
            sa = (1 + 15*T) * pga
        elif T <= 0.55:
            sa = 2.5 * pga
        else:
            sa = (1.36 * pga) / T
        sa_vals.append(sa)
    Sa_extended[label] = sa_vals

# Plot Final UHS
plt.figure(figsize=(8, 6))
for label, values in Sa_extended.items():
    plt.plot(periods, values, linewidth=2, label=label)

plt.title("Uniform Hazard Spectra of Saraighat Region for
Different Recurrence Intervals")
plt.xlabel("Period (Sec)")
plt.ylabel("Sa / g")
plt.xlim(0, 4)
plt.ylim(0, 0.9) # Reduceing Y-axis for better clarity
plt.grid(True, linestyle='--', alpha=0.6)
plt.legend(title="Return Period", fontsize=10)
plt.tight_layout()
plt.show()

```



METHODS TO PERFORM SITE SPECIFIC SEISMIC HAZARD ASSESSMENT (2).pdf

ORIGINALITY REPORT

19% SIMILARITY INDEX	15% INTERNET SOURCES	16% PUBLICATIONS	% STUDENT PAPERS
--------------------------------	--------------------------------	----------------------------	----------------------------

PRIMARY SOURCES

1	link.springer.com Internet Source	2%
2	www.researchgate.net Internet Source	1%
3	www.coursehero.com Internet Source	1%
4	noexperiencenecessarybook.com Internet Source	1%
5	bbs.huaweicloud.com Internet Source	1%
6	conf.ncree.org.tw Internet Source	1%
7	Satyaprakash Mishra, Aman Kumar, Arjun Sil. "Comprehensive seismic hazard assessment for Guwahati City, Northeast India: Insights from probabilistic and deterministic seismic hazard analysis", Natural Hazards Research, 2023 Publication	1%
8	tudr.thapar.edu:8080 Internet Source	<1%
9	Aman Kumar, Satyaprakash Mishra, Arjun Sil. "Seismic hazard mapping of Arunachal Pradesh: Integrating updated data and logic	<1%